sustainability

MDPI

Article

Pedestrian Single and Multi-Risk Assessment to SLODs in Urban Built Environment: A Mesoscale Approach

Graziano Salvalai [1], Juan Diego Blanco Cadena [1], Gessica Sparvoli [2], Gabriele Bernardini [2] and Enrico Quagliarini [2,*]

[1] ABC Department, Politecnico di Milano, 20133 Milan, Italy
[2] DICEA Department, Università Politecnica Delle Marche, 60131 Ancona, Italy
* Correspondence: e.quagliarini@staff.univpm.it

Abstract: Pedestrians are increasingly exposed to slow-onset disasters (SLODs), such as air pollution and increasing temperatures in urban built environments (BEs). Pedestrians also face risks that arise from the combination of the BE features, the effects of SLODs on the microclimate, their own characteristics (e.g., health and ability), and the way they move and behave in indoor and outdoor BE areas. Thus, the effectiveness of sustainable risk-mitigation solutions for the health of the exposed pedestrians should be defined by considering the overlapping of such factors in critical operational scenarios in which such emergency conditions can appear. This work provides an innovative method to define a BE-oriented pedestrian risk index through a dynamic meso-scale approach that considers the daily variation of risk conditions. The method is ensured by a quick-to-apply approach, which also takes advantage of open-source repositories and tools to collect and manage input data, without the need for time-consuming in situ surveys. The resulting risk conditions are represented through meso-scale maps, which highlight the risk differences between BEs by focusing on their open spaces as fundamental parts of the urban road network. The method is applied to a significant case study (in Milan, Italy). The results demonstrate the ability of the approach to identify key input scenarios for risk assessment and mapping. The proposed methodology can: (1) provide insights for simulation activities in critical BE conditions, thanks to the identification of critical daily conditions for each of the factors and for single and multiple risks and (2) support the development of design and regeneration strategies in SLOD-prone urban BEs, as well as the identification of priority areas in the urban BE.

Keywords: risk assessment; pedestrian behaviour; climate change; urban heat island; air pollution

Citation: Salvalai, G.; Blanco Cadena, J.D.; Sparvoli, G.; Bernardini, G.; Quagliarini, E. Pedestrian Single and Multi-Risk Assessment to SLODs in Urban Built Environment: A Mesoscale Approach. *Sustainability* **2022**, *14*, 11233. https://doi.org/10.3390/su141811233

Academic Editors: Fernando Fonseca, Paulo Ribeiro, Elisa Conticelli and George N. Papageorgiou

Received: 14 July 2022
Accepted: 22 August 2022
Published: 7 September 2022

1. Introduction

Pedestrians are increasingly exposed to the risks of slow-onset disasters (SLODs) such as air pollution and increasing temperatures while living in and moving around cities, and their perception is significantly influenced by the configuration of the urban built environment (BE) [1]. Urban landscapes are not formed by the individual landscape elements that make up the street; instead, they are formed by the mutual connections of multiple elements. For example, trees and green spaces, low building layouts, the aesthetic facades of streets and buildings, and open spaces function together to amplify the attractiveness of the space [2,3].

Urban areas, and therefore pedestrians, are particularly vulnerable to exposure to pollutants, as the urban form alters the microclimate and air quality [4], discouraging people from walking in cities and exposing them to risks depending on their individual characteristics (for example, age, health, ability). The condition is aggravated by the fact that pollutant sources are mainly concentrated in urbanized areas, such as vehicular traffic, industrial activities, heating systems, and commercial areas [3,5]. High pollutant emissions can cause severe damage to human health [6–8], and variations of its concentration levels

below the urban canopy could indicate the existence of specific, local, and contemporaneous anthropogenic sources that may be threatening the outdoor environmental quality.

Furthermore, cities are affected by the well-known phenomenon of the urban heat island (UHI) [9,10] due to their morphological peculiarities, land surface cover and usage, and lack of greenery. High UHI values compromise citizens' everyday commuting, open-air activities, and well-being in general [5]. Moreover, air pollution and increasing temperatures have been recognized by numerous studies as the most relevant SLODs because of the great impact they have on people's health and on BEs in the medium and long term [5,11,12]. In addition, they have a considerable correlation with other SLODs (e.g., glacial retreat, ocean acidification) [13].

Thus, investigating factors that influence behavioural responses, pedestrians' health and awareness of SLODs (social vulnerability and exposure) at the urban level is a paramount target for research and practices devoted to sustainable and resilient urban BE design and regeneration (physical vulnerability) [3,14].

1.1. Pedestrian and the Meso-Scale Level in SLODs: Roads Network

Roads networks are paramount components influencing the effect of SLODs, essentially because they organize the whole urban form, influencing pedestrian activities and behaviours (including walking) [14–18]. Road networks are the set of areas and paths for public use intended for the circulation of pedestrians and vehicles, characterized by different levels of connection and specific types of transport, and are crucial in the management, development, and growth of cities [14,17,19]. In these areas and paths, people live, work, and interact, thus playing a fundamental role in the public life of cities and communities.

According to previous classification approaches [20], the road network is composed of two main open spaces:

- Areal Spaces (ASs): e.g., squares. These are spaces that express the habitat of the city, as well as places to meet and aggregate. From the urban point of view, the square can be defined as a free space, partially or fully surrounded by buildings. The shape, the location, the function, and the aesthetic expression of the square historically follows urban evolution, in which the main functions of a place of passage, place of utility, or place of stay can be combined or entirely grouped together. The importance of the square further increases as an urban space if it includes civil or religious buildings that are part of a city's monumental heritage.
- Linear Spaces (LSs): Spaces of public use, identifiable as roads and streets, including those connecting ASs. They are often the most vital public spaces in cities.

Hence, a meso-scale approach to SLOD risk assessment, from the pedestrian perspective, can provide quick insights on the matter by defining common conditions for each of the elements comprising the road network (where pedestrians can be exposed while moving in Bes). The same approach has been commonly applied to other kinds of disasters, supporting a rapid analysis of risk by focusing on "hot-spots" in the whole urban fabric [21,22].

1.2. SLODs Risk from the Pedestrian Perspective

Research on SLODs has steered towards a deep examination of the BE, its features, and the way it adapts to weather variations and the behaviours of its population; additionally, the BE analyses consider the context and the temporal scale to provide evidence. These can be structured to fit and shape the unified concept of risk, which results from integrating hazard, exposure, and vulnerability [3,5,23,24].

The hazard would be determined by estimating the intensity of environmental forces resulting from the combination of the site contaminants and the environmental context [18,20,25]. Given the overall context regarding impacts on pedestrians and their tasks in the urban BE, the main SLODs hazards identified in this study are increasing temperature and air pollution. According to previous approaches [11,26], data collection of the main hazard conditions arising from air pollution and increasing temperature in the BE is made using

indexes such as the universal thermal climate index (UTCI) [27] and the air quality index (AQI) [28]. These can be used in a simplified manner, which requires rather commonly surveyed parameters to estimate the pedestrian's sensation of their surroundings.

Differently, exposure is focused on human presence (e.g., the total number of people, overcrowding probability) [29], which essentially changes over time and space depending on urban BE use in indoor and outdoor areas [11,29,30].

Meanwhile, vulnerability is related to the expected microclimates generated from the BE features (physical vulnerability) and their potential effects on the population immersed in it, based on their susceptibility (social vulnerability) [29]. Thus, physical vulnerability is linked to the geometric and physical characteristics of the BE that condition the local microclimate and is evaluated by distinguishing between the two SLODs taken into consideration (increasing temperature and air pollution) [3,5,9,10]. Instead, social vulnerability involves people and their sensitivity to events that may affect their health (deserving further studies), which is fundamental to the assessment of vulnerability [6,23,29,31–33]. According to the literature, different issues define social vulnerability as the result of social, economic, political, and cultural variables such as level of education, employment status, and income.

As pointed out by previous works in the context of SLODs [23], different groups of people (and so of pedestrians) depending on their social vulnerability can be classified according to the ability of their bodies to assimilate, balance and recover from the effects of increasing temperature and air pollution. This assumption considers the direct correlation between the exposed pedestrians and their sensitivity towards the risk source [2,3,6,18,31–33], which may vary depending on age groups (e.g., children, young people, adults, elderly) and health complications (e.g., respiratory, cardiac, or other pathologies). Such groups can be defined as [23]:

- Babies (0–5 years): their organs are still developing, and their immune system is not yet accustomed to certain critical conditions in the outdoor environment. In addition, paediatric diseases can easily become worse when babies are exposed to high temperatures and pollutants.
- Young people (6–18 years): the effects of SLODs are lower than those of babies due to their growth, but prolonged exposure to these conditions could still result in permanent damage.
- Elderly (+65): their vulnerability is essentially determined by their lifestyle. However, most of those people are less able to adapt to the stressful conditions in the environment. Prolonged exposure to specific hazards could increase the risk of death [34,35].
- Frail health: this group includes individuals with a particular health condition that may endanger them when they are exposed to certain hazards [36]. In particular, fragilities related to SLODs are: respiratory (e.g., asthma and allergies), cardiovascular and metabolic (diabetes) diseases and syndromes.
- Adults: this group can be assumed to include any other pedestrians not in the previous categories.

Previous works [5,13,23,24,37,38] have developed methods to analyse and recognize exposure, vulnerability and risk to SLODs in urban environments. However, the risk assessment of SLODs is a multivariable problem that can be investigated by deconstructing it according to the type of hazards involved and their interaction with exposed users and the BE.

The use of risk matrices has been proposed and studied by researchers and institutions to label, compare and acknowledge the risk of a certain situation, or a combination of settings [39,40]. In this sense, the risk matrix approach (RMA) [23,40–42] is one of the most interesting ones for real urban BE applications, mainly because: (1) it is robust and can be used with respect to a diverse range of risk assessments scopes and goals, and (2) it is a quick-to apply an approach that integrates, quantitative analysis (from large databases) and qualitative assessment (from experience and knowledge).

1.3. How to Improve Pedestrian SLODs Risk Assessment?

The main gaps in previous works concern the management of the relevant variables. Studies on the assessment of SLODs [5,37] and related risks through open-source approaches are based on the collection and processing of data from territorially fixed survey stations and do not consider local variations due to the different morphology of BE. This is crucial in considering the differences between different ASs and LSs, that is, physical vulnerability. Furthermore, the characterisation of the geometric and morphological layout of the road (dimensions of the roadway, presence of pavements and bike paths, etc.) [5,14,43], of green infrastructure (rows of trees, hedges, parks, etc.) [44–46], and traffic levels [17,24,36,47] has a strong impact on determining the effects of SLODs on pedestrian behaviour and habits, as well as their health as a fundamental component of the social vulnerability.

Previous studies [11,48] have represented the daily variations of the risk conditions, but less has been done in the management of risk data and overall conditions for ASs and LSs composing the real-world roads network. In this sense, the development of quick methods able to dynamically manage and represent (i.e., through maps) is one of the recommended steps to support stakeholders and decision makers to assess "hotspots" in the urban BE due to SLODs risks. Using a spatio-temporal approach could allow a direct comparison between: (1) the levels of vulnerability and exposure over space and time for each of the SLODs, thus identifying their variation and most critical conditions, and (2) the single SLODs risk that can coexist and be overlapped in the urban BE, thus moving toward a multi-risk perspective. Furthermore, this spatial representation allows decision-makers to map the single and multi-risk and identify the presence of target (i.e., sensitive) buildings in terms of vulnerability and crowding. Finally, focusing on ASs and LSs ensures pursuing a pedestrian-oriented standpoint on SLODs risk as well as a quick-to-apply approach relying on the effective meso-scale components of the urban BE [2,14,17].

1.4. Work Aims

In view of the above, this work is aimed at defining an innovative quick-to-apply method to define a BE-oriented pedestrians' risk index through dynamic maps that consider the daily variation of risk conditions of typical working days, for each BE element (LS or AS). The method pursues a single-risk or multi-risk approach at the meso-scale level. It first assesses each SLOD individually and then combines them into a single index.

This method uses open-source tools to collect and process the input data, without the need for on-site inspections and costly in situ surveys, by integrating existing tools and parameters to allow a more accurate pedestrian-oriented characterization of risk factors and outcoming single to multi-risk. Factors related to social vulnerability and exposure are managed by defining typological conditions for outdoor and indoor area uses. Building use classes have been innovatively defined through this work to support these analyses, based on the type of intended use and the pedestrians who use the space. Other pedestrian-related factors (i.e., the effects of traffic levels) are also being managed in innovative ways. Collected data concerning hazard, vulnerability and exposure are then combined according to a matrix-based approach through an hour-based assessment and by considering the urban form, both in single and multi-risk perspectives.

The proposed method is applied to a significant urban BE context to demonstrate its capabilities. In specific, Italy, in particular, its northern area (Piedmont, Lombardy and Veneto regions), is recognized as one of the most critical areas of central Europe in terms of exposure to SLODs risk for more or less long periods and have been labelled on the emergency events database (EM-DAT) [49] as a country affected by extreme temperatures. In addition, the world health organization (WHO) has recorded average annual concentrations of particulate matter (PM 2.5) beyond health limits for the metropolitan city of Milan [50,51]. Therefore, the method is thus applied to some LSs (i.e., urban canyons) and an AS (i.e., a square) in Milan, Italy. These elements of the road network are used for both

vehicles and pedestrians. The SLODs risk in Milan is also aggravated by being one of the most densely populated cities in Italy, hosting about 1 million people [52].

2. Phases, Materials and Methods

This work is organized in three phases, following the general workflow presented in Figure 1:

- *Physical vulnerability assessment* depending on the BE *geometric and morphological* characteristics and on its hazards. Open-source data collection tools are used to this end (Section 2.1). This phase defines two physical vulnerability indexes *Pv*, one for increasing temperature and one for air pollution, both organized in 5 classes in an RMA-based approach.
- *Exposure and social vulnerability assessment* depending, respectively, on the intended uses of buildings and open spaces in the BE, and on the groups of pedestrians (by age, by health fragilities) who can attend the B, (Section 2.2). This phase defines an exposure index *E* and a social vulnerability index *Sv*, both organized into 5 classes in the RMA-based approach.
- *Overall risk matrix assessment* by first combining *Pv*, *E* and *Sv* for each risk by itself, and then in a combined manner. Related meso-scale maps are also provided (Section 2.3).

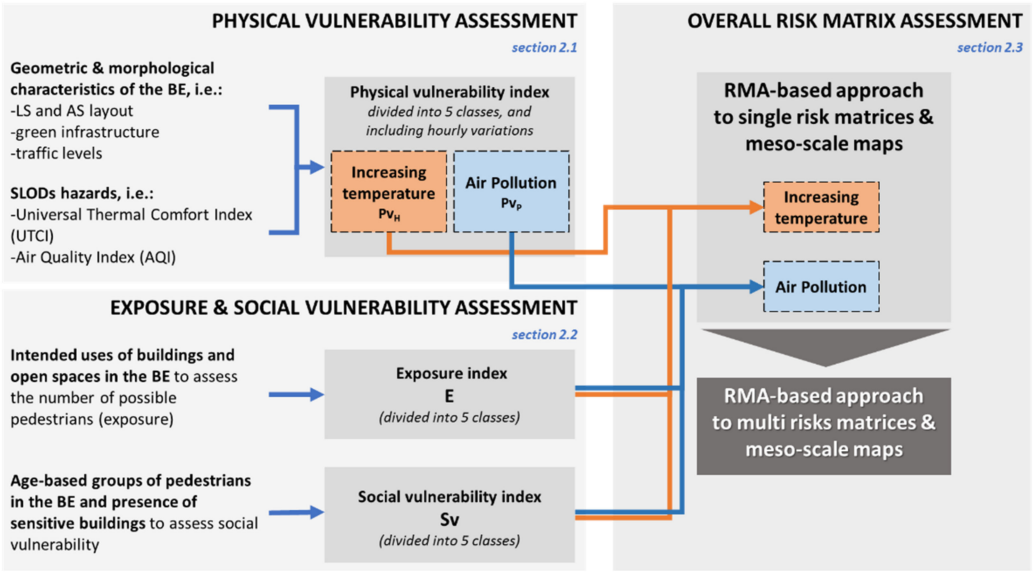

Figure 1. General operational framework representation for the definition of risk indexes, including references to the related methodological sections.

The proposed method takes advantage of vulnerability and exposure assessment techniques based on previous works [11,23,37], improving and adapting them to allow a faster and more effective assessment of BE as discussed in the following. All the work phases consider that the data collection is carried out mainly through open-source tools, preferable for the easy availability and applicability and however reliable for the adopted scale of observation. Both Pv_H values are unique for each AS/LS assessed, using the meso-scale approach [2,14,17], but they vary on an hourly basis based on some of their related factors.

Finally, the methodology is then applied to representative case studies in the city of Milan (Section 2.4).

2.1. Physical Vulnerability Assessment

The physical vulnerability assessment *Pv* relies on the collection and organization of the geometric and morphological characteristics of the BE [2,3,7,20,39] and hazard data, relating to the main sources of physical and physiological stress for pedestrians in the

urban BE (increasing temperature and air pollution) [2,3,7,20,39]. The process consists of two phases.

The first step concerns the application of the existing methods to collect morphological data on the BE [44], i.e., the main sizes of each LS and AS and the relationships between them (height/width ratio); the configuration of built fronts in terms of their symmetry and of the presence and quantity of nodes and connections on LSs and ASs (synthetically called permeability), so as to additionally identify the limits of each open space; the morphological structure in terms of geographical orientation of the LSs and Ass; and of the density of the urban form, that is, an index of the urban development of a certain area. The parameters described above can be collected through open-source tools such as Google Maps [53], which incorporates a measurement tool, and Google Street View, to deliver an overview of the BE.

The second step innovatively integrates this methodology by providing additional details in the following parameters:

- Road layout, defining the dimensions and function of features that characterize them, such as traffic dividers, vehicle lanes (trams, buses, etc.), sidewalks and bike paths [2,14,19,20,43]. Such kinds of data can be collected from the satellite maps of Google maps, using the special measurement tool provided on the website.
- The presence and type of green infrastructure (linear or areal), as it absorbs air pollutants, mitigates wind effects, and attenuates temperature rise and the intensity perceived by people [2,20,45]. The same sources for road design are used to collect these data.
- Reliable traffic levels [17], according to traffic data provided by online maps (Google Maps and OpenStreetMap) [53,54] provided by an existing methodology [47]. This method overcomes the problem of the accuracy of the simulations because it is based on direct observations of reality. The first step is the collection of data by observing Google Maps traffic maps at hourly intervals from Monday to Friday, considering the "Typical traffic" option that provides average traffic levels from 06:00 to 23:00. The period from 23:00 to 06:00 (not covered by Google Maps surveys) was regarded as homogeneous and corresponding to the lowest level of traffic recorded during the day. This simplification was considered acceptable because of the low level of traffic during the night-time and the absence of people on the road. Then, to allow a more accurate assessment, the road types were defined according to their importance in the urban network and the main geometric characteristics, using the same sources of the road layout parameters. Each road type can be correlated to the service range per lane, defined as the number of vehicles equivalent to the hour and therefore the total service range, as prescribed by the Highway Code, issued by the Italian Ministry of Infrastructure and Transport [55]. The final step is the recognition of the overall traffic model defined as the level of comfort (LoC) for drivers and represented in Table 1. Numerical values (0.2–1.2) were assigned to each level to allow a quantitative assessment in terms of the number of equivalent vehicles passing through the unit of journeys in one hour. This classification was made based on the six LOS (levels of services) defined by the highway capacity manual (HCM 1985-2022) [56], which evaluates the amount of traffic flows that will be able to travel the infrastructure under analysis, defined according to a pejorative scale from A to F to which comfort levels are assigned (remarkable-not perceived). For each open space detected, a single weekly profile is defined, taking into account the worst combination of those observed in working days. The approach provides a qualitative representation of traffic models on an hourly scale.

According to previous approaches [26,37], data on the main hazard conditions for air pollution and increasing temperature in the BE can be represented by indexes such as the universal thermal climate index (UTCI) [27] and the air quality index (AQI) [28]. They can also be used in a simplified manner, which requires rather commonly surveyed parameters to estimate the pedestrian's sensation of their surroundings.

Table 1. Levels of comfort (LoC). Classification of traffic conditions about the level of congestion of traffic, according to HCM guidelines.

Code	Description	Level of Comfort	Factor
A	Drivers do not suffer interference at their own gear, they have high possibilities of choosing the desired speeds (free).	Remarkable	0.2
B	The higher density compared to that of level A begins to be felt by drivers who suffer slight conditioning to the freedom of manoeuvre and the maintenance of the desired speeds.	Discreet	0.4
C	The freedom of travel of individual vehicles is significantly affected by mutual interference that limits the choice of speeds and manoeuvres within the current.	Modest	0.6
D	It is characterized by high density but still by the stability of outflow; speed and freedom of manoeuvre are strongly conditioned; modest demand increases can create problems with the regularity of travel.	Low	0.8
E	The average speeds of the individual vehicles are low (about half of those of level A) and almost uniform; there is practically no possibility of manoeuvring within the current; the motion is unstable since small increases in demand or small disturbances (slowdowns, for example) can no longer be easily reabsorbed by speed decreases and thus triggers congestion.	Very Low	1.0
F	The flow is forced: this condition occurs when the traffic demand exceeds the disposal capacity of the useful road section for which there are queues of increasing length, very low runoff speeds, and frequent stops of motion.	Unrecognize	1.2

To obtain a more realistic representation of the case studies, it is necessary to identify the sensors closest to each other and the studied area and collect, store and process data for at least one year of observation (including the period of interest) and then derive hourly profiles (for 24 h).

For increasing temperature, UTCI was assumed to be an indirect measure of the average surrounding intrinsic surface albedo material property, as it modifies the way solar radiation is distributed in the canyon, hence perceived temperature. In fact, UTCI defines the thermal comfort level of an environment through the combination of air temperature (°C), average radiant temperature (°C), wind speed (m/s) and relative humidity (%) or vapour pressure (hPa). Once the data from the closest sensors are obtained, UTCI is calculated using the method provided by the American Conference of Governmental Industrial Hygienists (ACGIH) [57] and the Universal Thermal Climate Index guidelines.

Likewise, AQI is easily estimated from data collected at air quality monitoring stations. The method is based on the suggested and current pollutant concentration in air of the main pollutants related to health effects: PM10 and PM2.5_respirable dust (<10 μm and <2.5 μm), NO2_nitrogen dioxide, O3_ozone, SO2_sulphur dioxide. The calculation method and the healthy concentration limits for exposed pedestrians follow those established by the Environmental Protection Agency (EPA) [58].

The physical vulnerability is then evaluated as a differentiated response of the BE to the SLODs. Increasing temperature and air pollution are, hence, first considered individually.

Table 2 shows the parameters considered in the physical vulnerability assessment, including their description and association with the values for calculating *Pv*, considering both increasing temperature and air pollution. A level of impact on the decrease in the severity is assigned to each of the physical vulnerability parameters, relying on a quick (range-based or descriptive) approach, by providing 4 levels moving from the best scenario condition to the worst one: High (H), Medium (A), Low (L), and None (N).

Table 2. Summary of the criterion adopted for the assessment of the levels of physical vulnerability, keeping the increasing temperature and air pollution separate.

Parameter	Description	Impact on the Decrease in Severity Levels	Impact on *Pv*
Increasing Temperature			
Green Cover	Includes the presence, type and effect of Green Infrastructures in the BE [46,59,60].	**H**: areal or linear green (mitigating and adaptive effect) **A**: linear green, direct shade on the road, especially on sidewalks (local effect) **L**: green areas, parks or green areas that do not have a direct effect on the road (shade) but still have a mitigating function (well on the scale of the neighbourhoods, less on the local scale of the canyon) **N**: no type of green infrastructures present	The presence of green impacts the hourly variation of physical vulnerability, especially in the daytime. Therefore, it is further integrated concerning the newly defined combination.
Albedo	The UTCI index [27] is used to assess the link between the external environment and human comfort [61].	**H**: comfort (until 26°) **A**: moderate stress (27–31°) **L**: strong stress (>32°)	This parameter is the dominant variable in the *Pv* assessment.
height/width ratio	The main dimensional ratios of the open spaces of the BE (geometry and morphological structure) are calculated, and then the temperature change and the orientation of the dominant direction of wind flow are assessed [62,63].	**H**: height/width ≈ 1 **A**: height/width < 1 **L**: height/width ≥ 2	This parameter defines the intermediate conditions of risk to be subdivided into three homogeneous subcategories.
Air Pollution			
Traffic	Levels of traffic (Section 2.1) are detected in the various streets of the open spaces considered, taking as reference the worst daily combination among those observed (working week) [24,36,47,64].	**H**: LoC REMARKABLE (code A) **A**: LoC DISCREET (code B) **L**: LoC MODEST (code C) **N**: LoC LOW or more (code D, E, F)	This parameter is the dominant variable in the *Pv* assessment.
Elements that capture pollutants	The density, spacing and position (in rows or parks) of the trees are evaluated. The presence of hedges, as a barrier between the road to the sidewalk [8,35,38].	**H**: hedges, trees with little thick crowns and well-spaced so as not to hinder wind flows (more pronounced effect in regular space, less in deep canyons) **A**: trees (same as "H") **L**: trees with dense foliage or lack of green	The elements that capture pollutants, in particular the presence of green infrastructure, play an important action mitigating the pollution produced by traffic. Therefore, it is further integrated concerning the defined combination.

Table 2. *Cont.*

Parameter	Description	Impact on the Decrease in Severity Levels	Impact on *Pv*
Morphology and wind speed	The relationship between morphology and orientation of open spaces (LS and AS) with wind direction. To assess whether the conditions are favourable or unfavourable to the dispersion of pollutants [7,24,65].	**H**: high buildings alternating with open spaces, parallel wind **A**: reduction in open spaces and lower buildings (continuous fronts) **L**: 45° wind or perpendicular to the dominant direction of the open spaces	This parameter defines the intermediate conditions of risk to be subdivided into three homogeneous subcategories.

The combination of the aforementioned parameters defines a certain level for the physical vulnerability index *Pv* related to the specific SLOD to consider, that is, Pv_H for increasing temperature and Pv_P for air pollution. As for the impact on the decrease in severity levels in Table 2, *Pv* is a non-dimensional value and is classified according to five classes of impact: I—Negligible; II—Low; III—Medium; IV—High; V—Extreme. The higher the impact level of impact of each parameter or any combination thereof, the lower the *Pv*. Each level is assigned a risk multiplier, ranging from 1 to 5, and assuming a discrete value. In addition, levels II to IV are subdivided into three homogeneous subcategories to delineate intermediate risk conditions (approximation interval equal to 0.33). Levels I and V are assigned a single score to apply a conservative approach to risk analysis for boundary conditions and related uncertainty effects.

The vulnerability assessment concerning the increasing temperature is mainly related to the structures, elements and specific materials characterizing the BE that affect the exposure of pedestrians to thermal stress [46,59,61,62]: green cover; albedo; and height/width ratio. The main combinations and related vulnerability classes are set out in Table 3. In particular, the presence of green infrastructure is a particularly influential parameter in the assessment of physical vulnerability, as it significantly affects the effects of both SLODs. Therefore, it can increase or decrease Pv_H values by 1 or 2 classes depending on its impact on the severity level, as shown in Table 3.

Table 3. Main combinations of vulnerabilities (depending on the parameter impact on the decrease in the severity levels as in Table 2) about the increasing temperature and associated multiplication factor for the *PvH* for risk assessment in RMA. If the case analysed is not among the common combinations, please refer to the following conditions: **a**—green cover = N increases *PvH* by 2 classes; **b**—green cover = L increases *PvH* by 1 class; **c**—green cover = H decreases *PvH* by 1 class.

Physical Vulnerability *PvH* Classes for Increasing Temperature	Common Combination of [Green Cover; Albedo; Height/Width Ratio]	Risk Multiplier for *PvH*
Negligible I	[H; H; H] [a,b] or [H; H; A] [a,b] or [H; H; L] [a,b]	1.00
Low II	[H; A; H] [a,b]	2.00
	[H; A; A] [a,b]	2.33
	[H; A; L] [a,b]	2.66
Medium III	[A; L; H] [a,c]	3.00
	[A; L; A] [a,c]	3.33
	[A; L; L] [a,c]	3.66
High IV	[L; L; H] [c]	4.00
	[L; L; A] [c]	4.33
	[L; L; L] [c]	4.66
Extreme V	[N; L; H] [c] or [N; L; A] [c] or [N; L; L] [c]	5.00

The vulnerability assessment, linked to air quality, depends mainly on the presence of air pollutants from various sources in the BE and in the neighbouring areas and the conditions governing its dissemination [5,7,24,38,47,64,66]: traffic; elements that capture

pollutants (especially green infrastructure); morphology and wind speed. As for green cover in Pv_H assessment, the elements that capture pollutants influence the final Pv_P assessment. Table 4 hence shows Pv_P classes according to the main combination of air pollution parameters by additionally considering that elements that capture pollutants can decrease or increase Pv_P values by 1 class depending on their impact on the severity levels.

Table 4. Possible combinations of vulnerabilities (depending on the parameter impact on the decrease in the severity levels as in Table 2) about air pollution with associated multiplication factor (*PvP*) for risk assessment in RMA. If the case analysed is not among the common combinations, please refer to the following conditions: **a**—elements that capture pollutants = L increases *PvH* by 1 class; **b**—elements that capture pollutants = H decrease *PvH* by 1 class.

Physical Vulnerability *PvP* Classes for Air Pollution	Common Combination of [Traffic; Elements that Capture Pollutants; Morphology and Wind Speed]	Risk Multiplier for *PvP*
Negligible I	[H; H; H] [a] or [H; H; A] [a] or [H; H; L] [a]	1.00
	[A; A; H] [a]	2.00
Low II	[A; A; A] [a]	2.33
	[A; A; L] [a]	2.66
	[L; L; H] [b]	3.00
Medium III	[L; L; A] [b]	3.33
	[L; L; L] [b]	3.66
	[N; L; H] [b]	4.00
High IV	[N; L; A] [b]	4.33
	[N; L; L] [b]	4.66
Extreme V	[N; L; H] [b] or [N; L; A] [b] or [N; L; L] [b]	5.00

The Pv_H and Pv_P hourly profiles are then organized to show the value changes over time for each BE.

2.2. Exposure and Social Vulnerability Assessment

The second phase of work allows the evaluation of exposure *E* and the social vulnerability *Sv* in the BE separately. According to [11], *E* can conservatively rely on the identification of critical conditions in the number of possible pedestrians hosted in the BE, which refers to the evaluation of peaks in exposure. Then, the characterization of the age group and the analysis of frail health (mainly related to sensitive buildings) allow the completion of the *Sv* assessment. Then, the following steps are used to quantify the number of pedestrians potentially exposed to SLODs and their vulnerability in time and space:

- *Identifying the use classes to be assigned to the buildings and the open spaces in the BE*: six use classes have been identified based on the use of the buildings and the categories of users attending these spaces. Buildings and urban spaces are grouped into improved homogeneous categories (from A to F), as shown in Table 5. Each category is defined according to the type of space, the open spaces or buildings, and the attractiveness and comfort of the urban space. Given the context of the case study (see Section 2.4), this work adopts local regulations (L.R. n. 12, 11 March 2005), which reflect the general intended uses of the BE. This assumption is suitable for assessments on the entire Italian territory but remains valid even for case studies outside the national borders sharing similarly intended use typologies and BE use features since the classification has also been based on definitions from previous research all over the World [67–72].
- *The detection of the use classes (Table 5) of buildings and open spaces in the BE and their spatio-temporal features*: where available, GIS tools could support and facilitate the labelling process. Google Maps can also provide data primarily on facilities open to the public and on production (i.e., offices, schools, hospitals, homeless centres, theatres, factories). In addition, for each public facility and commercial activity, this tool offers additional information, such as its name, address, and opening times. In this work, this analysis was conducted on working days to hypothesize the flow of pedestrians in

terms of residents (moving out from the area) and regular visitors or workers (moving into the area).

Table 5. Use classes categories representing a classification of the potential social vulnerability due to intended use of the space as defined by L.R. n.12, 11 March 2005, including examples, definition and related references, and operational codes for the case study application.

Category	Examples	Definition and References	Code
sensitive	Schools, nursing homes, social welfare facilities, hospitals, etc.	Buildings characterized by social- or healthcare-intended uses imply the concentration of sensitive users due to their age or health fragilities [6,72]. The position of these places in the BE implies a local increase in vulnerability as *frail health* are more susceptible to increasing temperature and climate change [67,68].	A
commercial	Shops, bars, restaurants, etc.	Particularly attractive urban spaces/buildings thanks to the activities that can be carried out and the opportunity to meet people [69]. The fact that such buildings are often air-conditioned makes them strategic for sensitive users [70,73].	B1
culture/ services	Universities, places of worship, culture and entertainment (churches, cinemas, theatres, museums, etc.), social services, sports services (gyms, sports centres), transport services (railway stations, airports, etc.)		B2
business	Banks, insurance, research centres, private offices, professional studios, etc.	Buildings for public use and open to the public. The management activities (offices) and of service to companies and persons offering specialized services (professional offices, specialized clinics, sector shops, etc.). The ideal density of people is less than that of commercial activities, and there are mainly workers.	C
production	Factories, local businesses, couriers, warehouses, construction sites, labs, workshops, etc.	Buildings mainly hosting private activities and, in any case, reserved for authorized occupants.	D
residential	Homes, colleges, monasteries, hotels, etc.	The position of the houses in the urban context and the construction characteristics are dominant in the exposure [67]. The guests are mainly residents or people who spend a lot of time in these spaces.	E
open spaces	Parks, squares, avenues, etc.	Open spaces are strongly influenced by weather, seasons, morphology and surface conditions. The intended uses of these spaces may vary on certain days of the week or seasons and change the crowding [71]: 1—Presence of events (markets, concerts, special events, etc.) 2—Everyday use	F

- *Estimating the maximum admissible occupancy in terms of the number of people (pp), for buildings and open spaces in the BE*: the geometrical characteristics of the adjacent buildings and open spaces intended were detected to determine the maximum number of pedestrians in the BE. In this sense, this work conservatively assumes that each user in the BE can be a potential pedestrian, thus being exposed to SLODs outdoors. BE users can be distinguished into indoor users, which are calculated as described below, and outdoor users, calculated by the method described in the next point. The occupant load factors (pp/m^2) of the Fire Prevention Code (D.M. 3 August 2015) are employed to calculate the number of people in the building according to a quick approach to exposure assessment, since it varies depending on the use classes, as also suggested by conservative approaches of previous works [11]. Table 6 provides a brief overview of occupant load factors for outdoor areas, based on their typology. The total area of each building/open space is calculated using the Google Maps measurement tool (which

allows calculating the areas directly on the map) and multiplied by the corresponding occupant load factor to obtain the maximum admissible occupancy.

- *Assessing the additional crowding level of outdoor spaces:* levels of services (LOSs) [3,74] are used to describe the presence of outdoor users, in particular, pedestrians using walking areas in the outdoor spaces, according to Section 2.1 analysis of the road layout [3,74]. Thus, this analysis attempts to include the additional burden in terms of people exposed as a result of walking activities that are not directly related to the use classes hosted within the evaluated BE. LOS A [75] (Table 6) is considered a reference for pedestrian areas to account for a standard area in which pedestrians can move freely without being restricted or influenced by others.

Table 6. Quick occupant load factor for outdoor areas used in this work, depending on their intended use.

Intended Use of Open Spaces	Description	Quick Occupant Load Factor
Carriageway	Areas implying exclusive use of vehicles.	0.0 pp/m^2
Pedestrian Areas	Areas for exclusively pedestrian use assumed considering a low level of crowding in ordinary conditions (LOS A), during daylight hours. Users of these areas are considered "external users only".	0.1 pp/m^2
Dehor	Generally related to outdoor areas of bars and restaurants.	0.1 pp/m^2

- *Estimating the temporal variations of people exposed in the BE:* the temporal variation of exposure is obtained considering the opening times of activities hosted in public buildings and open spaces described in Table 5 and the habits of the residents, according to the general rules of previous works [11]. The hourly values are then normalized for the maximum total value during the day, calculated between 0 and 1. In this way, these normalized values can also be used to directly compare the exposure profiles of the different LS or AS analysed. Then, pedestrian exposure *E* classes are divided into 5 classes, depending on the normalized value ranges, as represented in Table 7, thus assuming the same *Pv* number of classes for homogeneity purposes in the next RMA-based assessment tasks. It is worth emphasizing that this approach follows a conservative standpoint, in which we can assume that all the people hosted in the BE could potentially walk outside during each given daytime, thus being "potential" pedestrians.

Table 7. Pedestrian exposure *E* classes depend on the range of normalized exposure value, and the related risk multipliers for RMA tasks.

Pedestrian Exposure *E* Classes	Range of Normalized Exposure	Risk Multiplier for *E*
I	lower or equal than 0.2	1.00
II	0.2 (excluded) to 0.4 (include)	2.00
III	0.4 (excluded) to 0.6 (included)	3.00
IV	0.6 (excluded) to 0.8 (included)	4.00
V	0.8 (excluded) to 1.00 (included)	5.00

- *Assessing the social vulnerability in the BE:* according to Section 1.2 literature overview, people are divided into 5 categories according to their age, habits and health conditions. Population census data, which are be available online for the given area [11], are used to quickly assess the distribution of people depending on their age, thus calculating their number in respect of the total number of pedestrians in the BE (see above). The social vulnerability based on such demographic groups is firstly associated with the exposure values by providing each of them a weight (*w*) based on their susceptibility to such hazard according to Equation (1), thus improving previous methods [11]:

$$Svg = exp_b \times w_b + exp_y \times w_y + exp_e \times w_e + exp_{ad} \times w_{ad} \quad (1)$$

where exp_b is meant to have the normalized exposure of babies; exp_y is the normalized exposure of young people; exp_e is the normalized exposure of the elderly; exp_{ad} is the normalized exposure of adults; w_b is the weight associated with babies' vulnerability; w_y is the weight associated with young people's vulnerability; w_e is the weight associated with the elderly population's vulnerability; w_{ad} is the weight associated with adults' vulnerability. To calculate the weights of Equation (1), the analytic hierarchy process (AHP) was used [76]. The AHP is commonly used to objectively determine if the significance criteria assumed between different factors can be considered valid in relation to the consistency ratio. When this ratio is lower than 10%, the proposed weights are considered acceptable. The criteria for the assessment of social vulnerability are those outlined in Section 1 and summarized above. This assessment does not consider the category "frail health", as it does not directly depend on the age of the users, but on the presence of particular buildings, recognized as sensitive buildings (A in Table 5).

The general vulnerability profiles, obtained as a result of the weighted combination of such pedestrian categories according to Equation (1) and to the AHP results, are organized into five classes of social vulnerability with increasing intensity, as summarized in Table 8.

Table 8. Social vulnerability *Sv* classes depend on the values of social vulnerability intensity and the related risk multipliers for RMA tasks.

Social Vulnerability *Sv* Classes	Range of Social Vulnerability Intensity	Risk Multiplier for *Sv*
Negligible I	0 (included) to 0.25 (excluded)	1.00
Low II	0.25 (included) to 0.50 (excluded)	2.00
Medium III	0.5 (included) to 0.75 (excluded)	3.00
High IV	0.75 (included) to 1.00 (excluded)	4.00
Extreme V	1.00	5.00

Finally, the presence of people in frail health is treated with caution. *Sv* is hence firstly calculated according to Equation (1), but then the presence of at least one sensitive building in the considered BE determines an additional increase of 1 class for levels I to IV since it is considered a risk-increasing condition (thus without needing a detailed assessment of the hosted users).

Due to the dynamic perspective in risk assessment and exposure/social vulnerability data collection and management, it is worth underlying that the social vulnerability varies over space (i.e., at the mesoscale level, so for each analysed AS and LS) and time depending on the presence of pedestrians in each assessed BE. Thus, the hourly profiles of *E* and *Sv* are then organized to show the variations in the value over time, for each BE.

2.3. Overall Risk Matrix Assessment

Physical vulnerability, exposure and social vulnerability are combined using an RMA approach to obtain a variable risk index that varies throughout the day. The risk of increasing temperature and air pollution are first assessed separately (single risk) and then by combining the two SLODs (multi-risk).

Single and multi-risk assessments are performed using the general conceptual representation in Figure 2, which follows a three-dimensional approach as it follows the definition of Equations (2)–(4). Physical vulnerability *Pv* classes have been organized from left to right in accordance with Section 2.1 and increased pedestrian impacts. The other two 3D axes focus instead on pedestrian-related issues, which are exposure *E* (in the conceptual representation, laying on the same plane of *Pv*) and social vulnerability *Sv* (identifying each plane in the 3D representation).

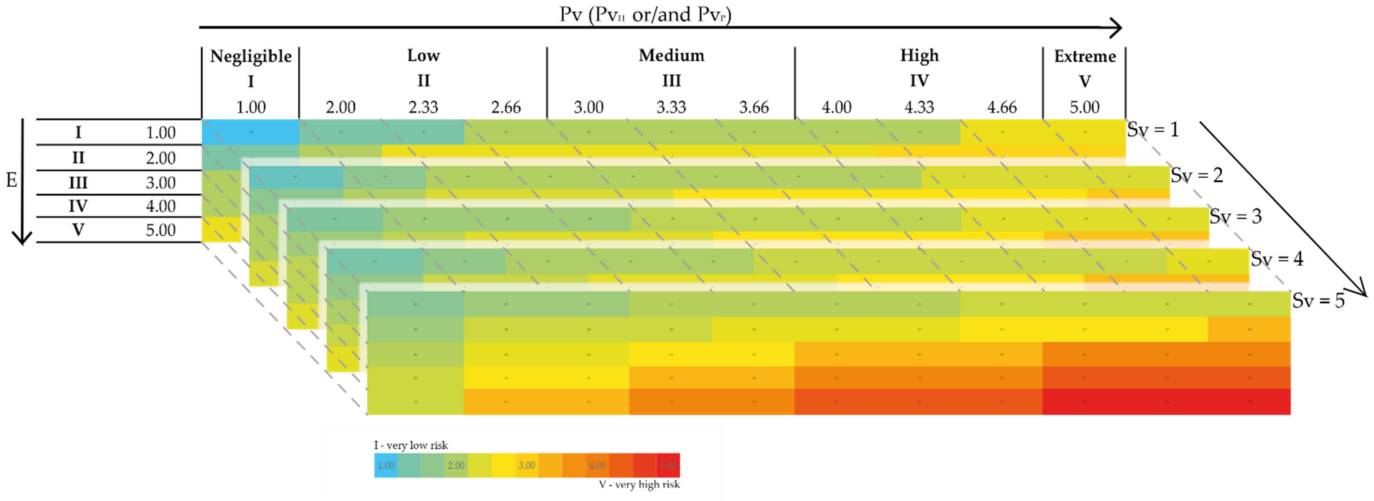

Figure 2. Conceptual representation of the RMA assessment in single and multi-risk scenarios. Cell values are calculated according to Equations (2)–(4), thus being correlated to a tridimensional matrix scheme. Values for the combination of *Pv*, *E* and *Sv* belonging to class V are conservatively approximated to 5. The colour bar for risks (bottom part) represents the principal calculated values rounded up to the nearest 0.33 multiple, being homogeneous with the *Pv* classification ranges.

The single (R_H for increasing temperature and R_P for air pollution) and multi-risk (R_{mhz}) values are calculated by multiplying the risk coefficients corresponding to each parameter and by taking the cubic root of the result, as shown by Equations (2)–(4):

$$R_H = \sqrt[3]{(Pv_H \times E \times Sv)} \quad (2)$$

$$R_P = \sqrt[3]{(Pv_P \times E \times Sv)} \quad (3)$$

$$R_{mhz} = \sqrt[3]{((Pv_H \times w_H + Pv_P \times w_P) \times E \times Sv)} \quad (4)$$

where Pv_H is associated with the multiplier of physical vulnerability related to the increasing temperature defined in Section 2.1 (Table 2); Pv_P is associated with the multiplier of the physical vulnerability related to the air pollution defined in Section 2.1 (Table 3); E is associated with the multiplier of exposure classes calculated in Section 2.2 (Table 7); Sv is associated with the multiplier of the social vulnerability calculated in Section 2.2 (Table 8); w_H is the weight related to the criticality of increasing temperature hazard; and w_P is the weight related to the critically air pollution hazard. w_H and w_P can be assumed depending on specific assumptions on which SLODs can be more critical in the considered scenario, as well as on the priority SLOD to be faced by the decision-makers. The cubic root assumption has the main purpose of maintaining the final risk a number between 1 and 5, thus according to the levels of the parameters involved.

Thus, the values of the risk index in Figure 2 are associated with a colour scale, from minimal to extreme risk, into homogeneous colour classes rounded up to the nearest 0.33 multiple according to the *Pv* classes. This colour scale is used to represent risks using a mixed space-time model based on urban maps. The representation was made assuming a uniform distribution of the risk index for each open space examined (LS or AS). The maps overlap the risk index classification to the position of sensitive buildings (use classes A), since they are characterised by the potential presence of fragile people, and special buildings (use classes B2), since they can locally increase the exposure by attracting large crowds.

The daily evolution of the risk scenarios was represented in the application case studies by considering the following homogeneous conditions over time depending on common pedestrian habits: morning (08:00–13:00), afternoon (14:00–19:00), evening (20:00–01:00),

and night (02:00–07:00). For each of these, the peak risk scenario, the maximum value computed using the risk matrix, was considered.

2.4. Presentation of the Case Study

Milan (Italy) is a representative case study to assess the contemporary phenomena of increasing temperatures and air pollution hazards in a densely populated metropolis. At the meso-scale, the neighbourhoods of Città Studi and Piazzale Loreto (Figure 3) are considered in this work as areas of due to:

- Average concentration of sensitive population (over 65 and under 5) and a fair concentration (highest in Città Studi) of schools and accommodation facilities for the elderly and disabled.
- Heavy density of public transportation.
- Proximity to stations that allow one to monitor the trend of temperatures (5 weather stations distributed on the territory of the municipality of Milan [77]) and stations for air quality control (7 Air Quality Station [78]).
- Low level of risk-mitigation strategies implemented due to low green coverage and high-level building density [79].

Città Studi is mainly characterized by different types of ASs and LSs, composing different classes of urban canyons in terms of BE characterization given in Section 2.1. Piazzale Loreto is an area under continuous evolution from the urban, economic and social points of view, and it is a relevant intersection of roads of different importance and use (mainly driveway use, with large sidewalks).

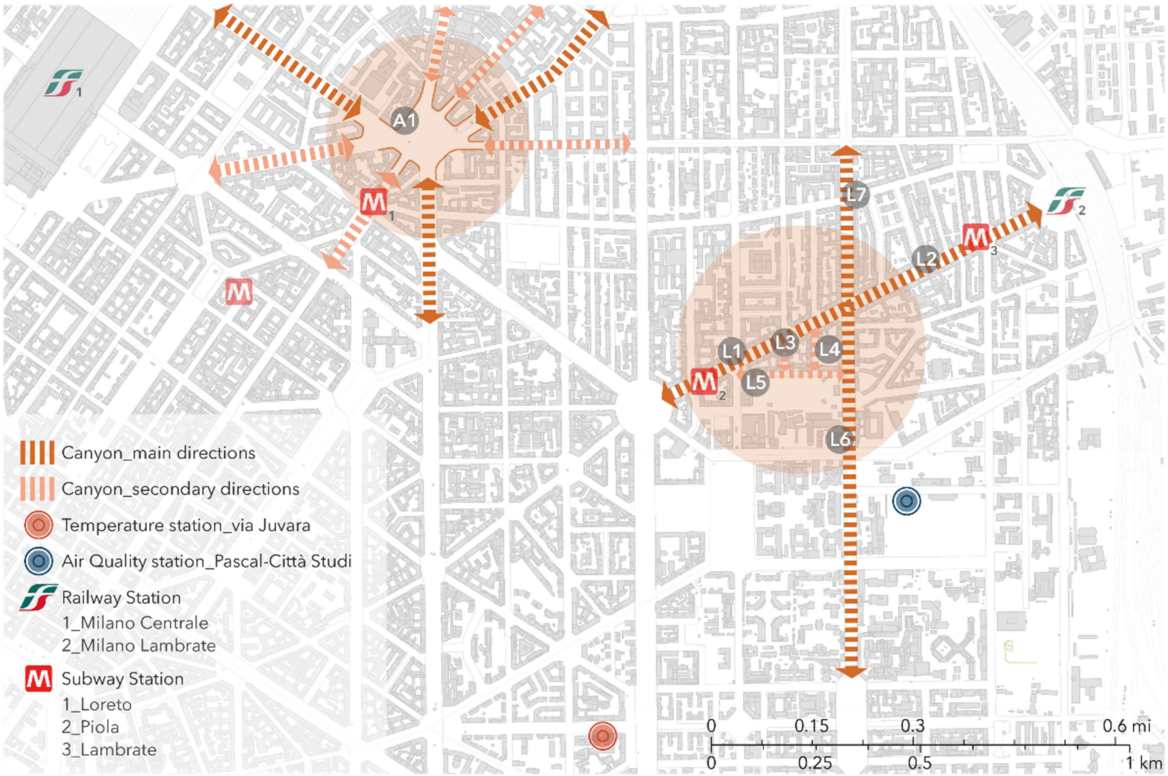

Figure 3. The case study area (Città Study on the right and Piazzale Loreto on the left) with the identification of ARPA survey stations used to collect data on air pollution and increasing temperature. The linear space (urban canyon) and the areal space (square) are: L1-via Pacini SO; L2-via Pacini NE; L3-via Orcagna; L4-via Fossati; L5-via Zanoia; L6-via Ponzio; L7-via Teodosio; A1-piazzale Loreto. Based on the GIS map freely available at geoportal of the municipality of Milan [80], elaborated by the authors.

The data collected from Google Maps [53] and the geoportal of the municipality of Milan [80] include the identification and qualification of buildings and open spaces in the BE, and the hourly variance of the presence of pedestrians depending on their intended use and the traffic flow during the day. The collection campaign was carried out between 20 May 2021 and 14 June 2021. In this period, the city of Milan, like all of Italy, was subject to restrictions regarding the crowding and opening hours of activities for reasons related to the containment of the effects of the COVID-19 pandemic [81,82]. Although this situation has affected the result as regards the presence of people in the evening and night, the application of the proposed method could be considered valid to test the process, since all the input data were collected to provide the risk index.

For the selected case studies, the environmental data were extracted by the regional environmental monitoring agency ARPA [77,78], which freely shares its measurement database of environmental monitoring, retrieving air quality data from the station of Pascal-City Studies and meteorological data from the station in via Juvara, which are the stations closest to the sites studied and equipped with the greatest number of sensors. The data were collected for a period of at least one year (increasing temperature: 2020, air pollution: 2017–2020), while the daily profile was obtained by averaging for each of the 24 h that make up a day.

3. Results

The application of the proposed method to the specific LSs and ASs in the Milan case study is discussed above, in accordance with the methodological framework (compare Figure 1). Table 9 shows the main characteristics of each LS and AS, as identified in the urban layout of Figure 3, according to the related parameters shown in Tables 2 and 5. Then, the results on hazard and physical vulnerability are resumed in Section 3.1, those on exposure and social vulnerability and shown in Section 3.2, and the final risk indexes are reported in Section 3.3.

Table 9. Synthesis of the main ASs and LSs characteristics considered through the criteria described in Tables 2 and 5.

		Case Study							
Parameter	**Characteristic**	**L1**	**L2**	**L3**	**L4**	**L5**	**L6**	**L7**	**A1**
Green Cover	Type of green infrastructure (areal)	Green park and trees	Green park and trees	-	-	Green park and trees	Green park and trees	Green park and trees	Green park and hedges
	Type of green infrastructure (linear)	Trees	Trees	-	-	-	Trees	-	Trees
Height/width ratio		0.80	0.80	0.80	0.80	1.00	0.40	0.70	0.21
Morphological Structure	Geographical Orientation	SO-NE	SO-NE	N-S	N-S	O-E	N-S	N-S	-
Traffic	Type of road	Two-way	Two-way	One-way	One-way	One-way	One-way	Two-way	Both
	LoC (max)	D	D	D	C	C	C	C	C
Elements that capture pollutants (trees and hedges)		Deciduous trees	Deciduous trees	-	-	Deciduous trees	Deciduous trees	Deciduous trees	Hedges
Use classes		B1, B2, C, E	B1, B2, C, E	A, B2, E	A, B2, E	E, F	A, B1, B2, C, E, F	B1, B2, C, D, E	B1, B2, C, E, F

3.1. Hazard Estimation and Physical Vulnerability

The hourly thermal stress was estimated by defining the universal thermal comfort index UTCI. According to Section 2.4, the case study analysis screened the week starting from of 24 July until 1 August, which was identified as the most intense heat wave of that year. As expected during the summer, the coincidence between these two SLODs implies the need to consider the multi-risk scenario to evaluate the worst health situation for pedestrians.

Considering the parameters affecting the physical vulnerability to increasing temperature, it is worth noticing that, in the selected case studies, the presence of green

infrastructure is almost exclusively limited to rows of trees along the streets, which provide shade to pedestrians who populate the paths.

The influence of geometry and orientation is mainly associated with the beneficial effect of the wind breeze, which, when parallel to the dominant dimension of open space, can promote the dispersion of heat.

Among the LSs in the area, the optimal situation from this point of view occurs in via Ponzio and via Teodosio, which have a low height/width ratio and wind parallel to the dominant direction. Other LSs that have the same orientation, as Via Orcagna and Via Fossati, cannot fully exploit the beneficial effects of the wind because they are too short and compact, so the heat is not able to disperse. In these cases, the lack of green infrastructure makes the situation even worse.

In terms of air pollution, the dominant parameter is the definition of everyday traffic, measured in each BE. Again, the presence of elements that capture pollutants, particularly green infrastructure, is assessed. In this case, according to the results, the main beneficial effects are related to the presence of hedgerows. When placed between sidewalks and roadways, they provide a barrier for the particles suspended at human height. This type of element is, however, scarce in the selected case studies, while there are many trees, which instead have beneficial effects on the improvement of air quality only if well-arranged and with the foliage suitably spaced, so as not to prevent the dispersion of particles.

In view of the above, and as shown in Figure 4, the worst situation in terms of physical vulnerability occurs for both SLODs in Piazzale Loreto, given: (1) no type of green infrastructure; (2) geometry characterized from a very low height/width ratio, without high and continuous fronts that do not favour the dispersion of heat and pollutants; and (3) an increased negative impact due to high intensity of traffic. On the contrary, via Teodosio and via Ponzio are the least vulnerable cases, thanks to: (1) the presence of well-distributed rows of trees; (2) the orientation favourable to the direction of the dominant wind (recorded by the meteorological station of Via Juvara); and (3) the configuration of built fronts, interspersed with large open spaces. According to the quick approach in data collection, such insights are rapidly and easily provided by a direct visualization of the BE on Google Street View.

3.2. Exposure Peak and Social Vulnerability

The daily variation in exposure profiles is clearly linked to the lodger function of the buildings in the assessed BEs. In the case of Città Studi, some built areas have predominantly residential uses. The profiles obtained in Figure 5a–c,g is generally characterized by a higher number of people present early in the morning and in the evening. This trend represents the possible movement of pedestrians going in and out, or visiting restaurants and open bars in the area. Figure 5d–f shows a different trend in peak exposure profiles because they refer to LSs characterized by the presence of large public buildings and outdoor spaces that are open from morning to late afternoon. In this regard, subway and train stations attract a great number of visitors and workers from early morning to late afternoon. Similarly, other attractive intended uses imply significant exposure in the BEs. In particular, via Pacini and via Teodosio are characterized by many shops, bars and restaurants, and, due to this, they are almost always crowded (Figure 5a,b). For instance, Piazzale Loreto (Figure 5h) is a mainly commercial/directional AS, but the presence of large residential buildings implies high exposure throughout the day. On the contrary, data concerning via Ponzio are mainly affected by the presence of university buildings and of sensitive buildings, which compose most of the intended uses along the LS sides, thus affecting peak conditions during the central time of the day, when such buildings are open to the public.

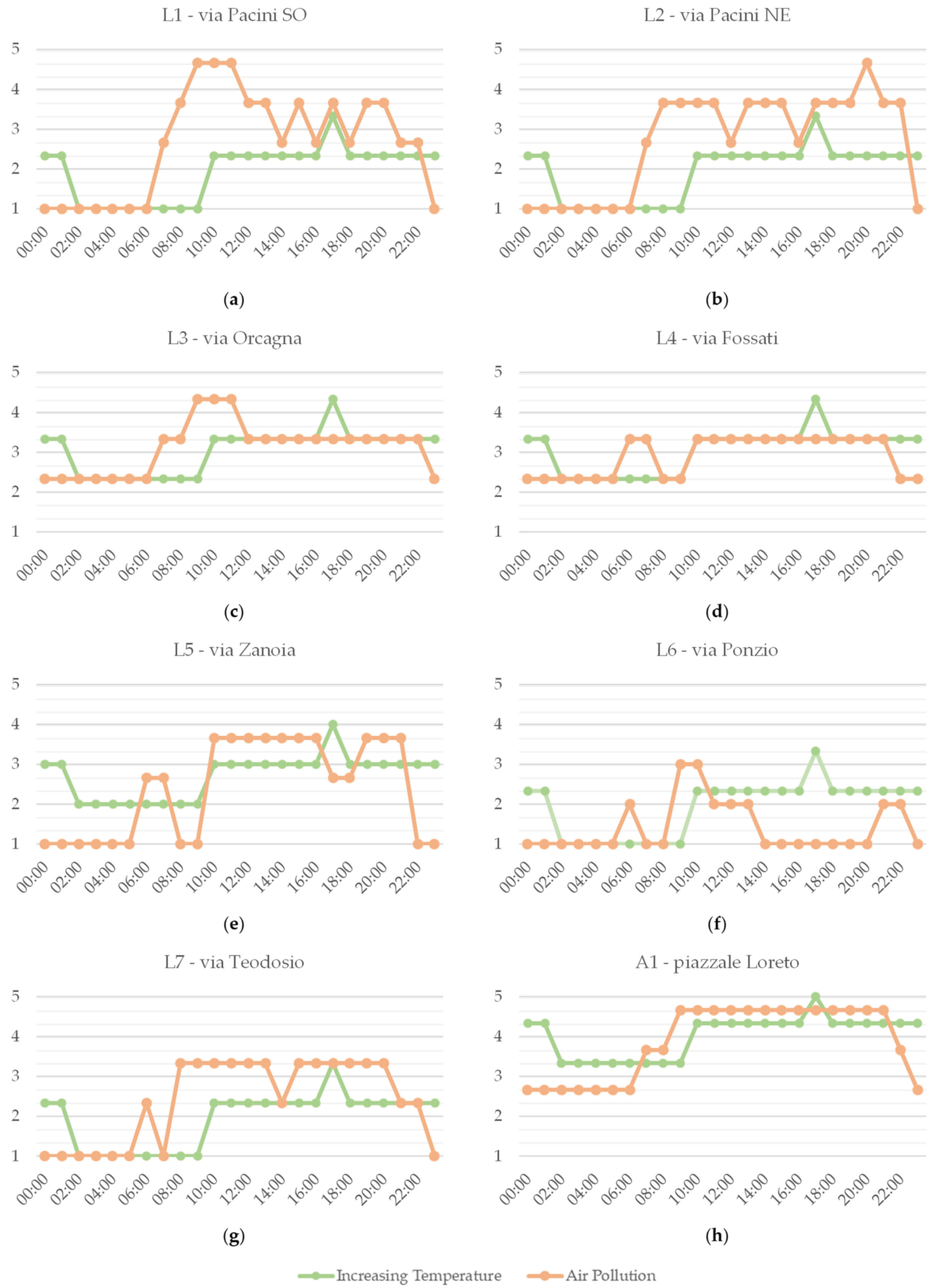

Figure 4. Hourly profiles of physical vulnerability to increasing temperature and air pollution for each of the areas in Figure 3: (**a**) L1—via Pacini SO; (**b**) L2—via Pacini NE; (**c**) L3—via Orcagna; (**d**) L4—via Fossati; (**e**) L5—via Zanoia; (**f**) L6—via Ponzio; (**g**) L7—via Teodosio; (**h**) A1—piazzale Loreto.

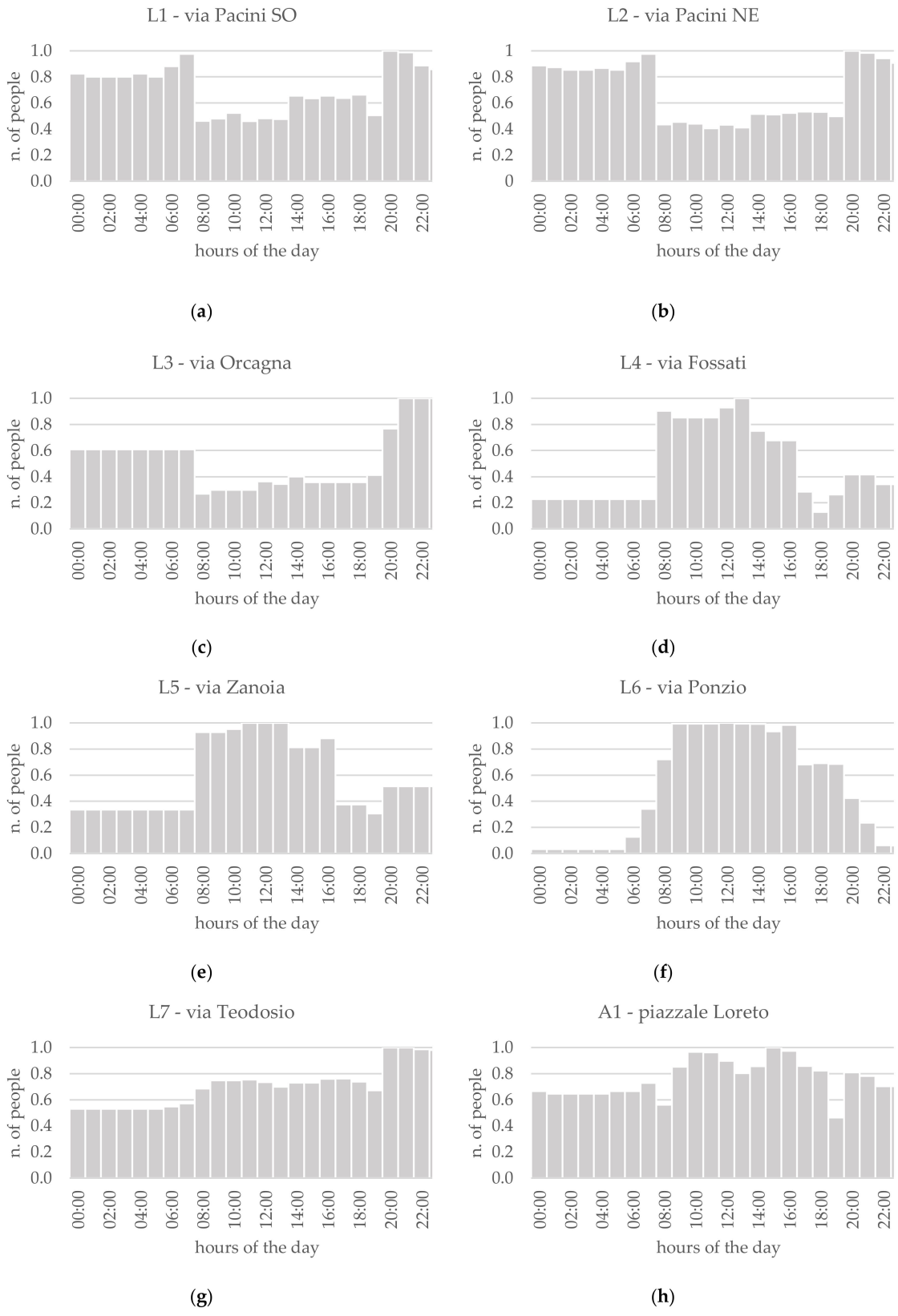

Figure 5. Hourly profiles of exposure (in terms of normalized exposure) for each of the areas in Figure 3: (**a**) L1—via Pacini SO; (**b**) L2—via Pacini NE; (**c**) L3—via Orcagna; (**d**) L4—via Fossati; (**e**) L5—via Zanoia; (**f**) L6—via Ponzio; (**g**) L7—via Teodosio; (**h**) A1—piazzale Loreto.

Concerning social vulnerability, data on the distribution of the population obtained by the SISI [83] of the Municipality of Milan confirm the general trend toward the ageing of the Italian population. The population of the districts of Città Studi and Piazzale Loreto (Table 10) are 22% elderly, while children and young people are 16%.

Table 10. Population resident (date: 31 December 2020) in Milan, proportions by functional classes. Source: SISI—Integrated Statistical System of the Municipality of Milan.

Functional Classes	Target (Age)	%
Babies	0–5	5%
Young People	6–18	11%
Adults	19–64	62%
Elderly	65+	22%

Considering previous works outcomes as discussed in Section 1.2 [6,13,32–36,68], the AHP-based assessment of social vulnerability described in Section 2.2 has been performed according to the following assumptions: (1) the elderly and babies are more susceptible than healthy adults when subjected to such conditions; (2) young people are less susceptible to the effects of SLODs than babies, as their bodies are more developed and more resistant to danger. Then, the AHP has been used to evaluate the reliability of literature criteria in Section 1, and the following weights are retrieved and applied to Equation (1) for the considered age classes:

- w_b = 0.45
- w_y = 0.20
- w_e = 0.31
- w_{ad} = 0.04

An acceptable consistency ratio equal to 2.5 < 10% was associated with these weights. Figure 6 summarizes the social vulnerability profiles according to the AHP assessment, and thus depending on the behavioural dynamics of pedestrians, which are based on the exposure profiles and the age statistics in Table 7. The critical values of social vulnerability profiles are concentrated in the central hours of the day, due to the contemporary presence of residents and non-residents, which imply the peak conditions in the exposure profiles. In BEs characterized by mainly residential use, as via Pacini, via Orcagna and via Teodosio, social vulnerability reaches high values late in the evening and early in the morning, confirming the trends in the exposure profiles. In the overall context of Figure 6, although the elderly are associated with a lower vulnerability coefficient than babies (see w_e), they have the greatest impact on Sv because of their number.

Considering the specific assessed BEs, Figure 6a,b shows high levels of vulnerability throughout the day due to the constant presence of pedestrians for all 24 h, which depends on the trends of related exposure profiles in Figure 5. Increasing values of vulnerability are registered in the second part of the morning (e.g., from 11:00 to 14:00) and when babies and young people are back from school and shops and public structures begin to open (i.e., from 15:00 to 17:00). In the late evening and at night, social vulnerability affects residents almost exclusively, including adults returning to their homes.

Figure 6d–f shows important peaks in Sv between 08:00 and 17:00. This trend depends on the presence of numerous public buildings that are open during the daytime. Some of these public buildings are sensitive buildings (class A in Table 5) and therefore determine an increase in Sv due to the expected presence of sensitive users (i.e., Faes school complex in via Ponzio and via Fossati; the neurological institute "Carlo Besta" and the national cancer institute in via Ponzio).

Figure 6. Vulnerability hourly profiles including the sensibility of the considered demographic groups (babies, young people, elderly, adults and frail health) for each of the areas in Figure 3: (**a**) L1—via Pacini SO; (**b**) L2—via Pacini NE; (**c**) L3—via Orcagna; (**d**) L4—via Fossati; (**e**) L5—via Zanoia; (**f**) L6—via Ponzio; (**g**) L7—via Teodosio; (**h**) A1—piazzale Loreto.

3.3. Risk Index

Figure 7 shows the single (Figure 7a for increasing temperature; Figure 7b for air pollution) and multiple (Figure 7c) risk indexes for the areas of activity examined in this work. In the multi-risk assessment, both SLODs were considered to have an equal impact on pedestrian health, so that weights assigned to calculate the multi-risk analysis (see Equation (4)) are, respectively:

- $w_H = 0.50$
- $w_P = 0.50$

From a general standpoint, from both single and multi-risk perspectives, the highest-risk value is reported for central hours during the day, in which most residents present in the studied area are elderly, babies and young people, and there are many non-residents of different ages and sensitivities. However, the main differences and similarities between increasing temperature and air pollution risks can be noted.

Figure 7a highlights that BEs characterized by the presence of green infrastructure (i.e., trees) are generally characterized by a lower risk of increasing temperature, even if they are heavily populated. In this sense, for instance, compare the conditions of via Pacini with those of via Ponzio, in accordance with Sections 3.1 and 3.2.

In terms of air pollution, Figure 7b shows that the riskiest BEs are those where traffic levels are particularly intense and where effective countermeasures are not available, such as for Piazzale Loreto. In the LSs placed in Città Studi, the risk is almost homogeneous because the main LSs (via Pacini, via Teodosio, via Ponzio) are crossed by rows of trees that dampen pollution.

Figure 7c represents the risk resulting from the combination of the two SLODs analysed above. In the middle of the day, between 11:00 and 17:00, pedestrians are just too high a risk because of overlapping critical conditions for both the SLODs. Such a result is especially evident for BEs characterized by the presence of numerous commercial activities and utilities (e.g., via Pacini, via Teodosio). It is interesting to note that high-risk values are found where residential use is particularly dense (e.g., via Orcagna, via Pacini, via Teodosio), especially in the evening (20:00–22:00) when most pedestrians in the BE are residents. In this regard, the role of Table 5 is very important, which allows one to classify the buildings present according to the classes of use and then to identify the type of users present in an area and the respective vulnerability to age and psycho-physical characteristics. In particular, in the case studies mentioned above, the use class *E* (residential) is dominant, and this results in the presence of people of all ages, in particular in the evening and night, and elderly people and children in the middle of the day.

Increasing Temperature_Risk

	02:00	03:00	04:00	05:00	06:00	07:00	08:00	09:00	10:00	11:00	12:00	13:00	14:00	15:00	16:00	17:00	18:00	19:00	20:00	21:00	22:00	23:00	00:00	01:00
via Pacini SO	3.00	3.00	3.00	3.00	3.00	3.00	2.67	2.67	3.33	3.33	3.33	3.33	3.67	3.67	3.67	4.33	3.67	3.33	4.00	4.00	4.00	4.00	4.00	4.00
via Pacini NW	3.00	3.00	3.00	3.00	3.00	3.00	2.33	2.33	3.33	3.00	3.33	3.00	3.33	3.33	3.33	3.67	3.33	3.33	3.67	3.67	3.67	3.67	3.67	3.67
via Orcagna	3.33	3.33	3.33	3.33	3.33	3.33	2.67	2.67	3.00	3.00	3.00	3.00	3.33	3.00	3.00	3.00	3.00	3.33	4.00	4.33	4.33	4.33	3.67	3.67
via Fossati	2.33	2.33	2.33	2.33	2.33	2.33	4.00	4.00	4.67	4.67	4.33	4.33	4.00	3.67	3.67	2.67	1.67	2.67	3.00	3.00	2.67	2.67	2.00	2.00
via Zanoia	2.33	2.33	2.33	2.33	2.33	2.33	4.00	4.00	4.33	4.33	4.33	4.33	4.33	4.33	4.33	2.67	2.67	2.67	3.00	3.00	3.00	3.00	2.67	2.67
via Ponzio	1.00	1.00	1.00	1.00	1.00	2.00	2.67	3.00	4.00	4.00	4.00	4.00	4.00	4.00	4.00	4.00	3.67	3.67	3.00	2.33	1.33	1.33	1.33	1.33
via Teodosio	2.33	2.33	2.33	2.33	2.33	2.33	2.67	2.67	3.67	3.67	3.67	3.67	3.67	3.67	3.67	4.00	3.67	3.67	3.67	3.67	3.67	3.67	3.00	3.00
piazzale Loreto	3.00	3.00	3.00	3.67	3.67	3.67	3.33	4.33	4.67	4.67	4.67	4.67	4.67	4.67	4.67	4.67	4.67	3.67	4.33	4.00	4.00	4.00	4.00	3.33

(**a**)

Air Pollution_Risk

	02:00	03:00	04:00	05:00	06:00	07:00	08:00	09:00	10:00	11:00	12:00	13:00	14:00	15:00	16:00	17:00	18:00	19:00	20:00	21:00	22:00	23:00	00:00	01:00
via Pacini SO	3.00	3.00	3.00	3.00	3.00	4.33	4.00	4.33	4.33	4.33	4.00	4.00	4.00	4.33	4.00	4.33	4.00	4.00	4.67	4.33	4.33	3.00	3.00	3.00
via Pacini NW	3.00	3.00	3.00	3.00	3.00	4.00	3.67	3.67	3.67	3.33	3.33	3.33	3.67	3.67	3.33	3.67	3.67	3.67	4.67	4.33	4.33	3.00	3.00	3.00
via Orcagna	3.33	3.33	3.33	3.33	3.33	3.67	3.00	3.00	3.00	3.00	3.00	3.00	3.33	3.00	3.00	3.00	3.00	3.33	4.00	4.33	4.33	3.67	3.33	3.33
via Fossati	2.33	2.33	2.33	2.33	2.33	2.67	4.67	4.00	4.00	4.67	4.33	4.33	4.00	3.67	3.67	2.67	1.67	2.67	3.00	3.00	2.33	2.33	2.00	2.00
via Zanoia	1.67	1.67	1.67	1.67	2.33	2.33	3.00	3.00	4.33	4.33	4.33	4.33	4.33	4.33	4.33	2.33	2.33	2.67	3.00	3.00	2.00	2.00	1.67	1.67
via Ponzio	1.00	1.00	1.00	1.00	1.33	2.00	2.67	4.33	4.33	4.00	4.00	4.00	3.00	3.00	3.00	2.67	2.67	2.67	2.33	2.33	1.33	1.00	1.00	1.00
via Teodosio	2.33	2.33	2.33	2.33	3.00	2.33	4.00	4.00	4.00	4.00	4.00	4.00	3.67	4.00	4.00	4.00	4.00	4.00	4.33	3.67	3.67	3.00	2.33	2.33
piazzale Loreto	3.00	3.00	3.00	3.33	3.33	3.67	3.33	4.67	4.67	4.67	4.67	4.67	4.67	4.67	4.67	4.67	4.67	3.67	4.33	4.00	3.33	3.33	3.33	3.00

(**b**)

Figure 7. *Cont.*

Multi-Risk

	02:00	03:00	04:00	05:00	06:00	07:00	08:00	09:00	10:00	11:00	12:00	13:00	14:00	15:00	16:00	17:00	18:00	19:00	20:00	21:00	22:00	23:00	00:00	01:00
via Pacini SO	3.00	3.00	3.00	3.00	3.00	3.67	3.33	3.67	4.00	4.00	3.67	3.67	4.00	4.00	4.00	4.33	4.00	3.67	4.33	4.00	4.00	3.67	3.67	3.67
via Pacini NW	3.00	3.00	3.00	3.00	3.00	3.33	3.33	3.33	3.33	3.00	3.33	3.00	3.33	3.33	3.33	3.67	3.33	3.33	4.33	4.00	4.00	3.33	3.33	3.33
via Orcagna	3.33	3.33	3.33	3.33	3.33	3.33	2.67	3.00	3.00	3.00	3.00	3.00	3.33	3.00	3.00	3.00	3.00	3.33	4.00	4.33	4.33	4.00	3.33	3.33
via Fossati	2.33	2.33	2.33	2.33	2.33	2.33	4.33	4.00	4.33	4.67	4.33	4.33	4.00	3.67	3.67	2.67	1.67	2.67	3.00	3.00	2.33	2.33	2.00	2.00
via Zanoia	2.00	2.00	2.00	2.00	2.33	2.33	3.33	3.33	4.33	4.33	4.33	4.33	4.33	4.33	4.33	2.67	2.33	2.67	3.00	3.00	2.67	2.67	2.33	2.33
via Ponzio	1.00	1.00	1.00	1.00	1.33	2.00	2.67	4.00	4.33	4.00	4.00	4.00	3.67	3.67	3.67	3.33	3.00	3.00	2.67	2.33	1.33	1.33	1.33	1.33
via Teodosio	2.33	2.33	2.33	2.33	2.67	2.33	3.33	3.33	3.67	3.67	3.67	3.67	3.67	3.67	3.67	4.00	3.67	3.67	4.00	3.67	3.67	3.33	2.67	2.67
piazzale Loreto	3.00	3.00	3.00	3.33	3.33	3.67	3.33	4.33	4.67	4.67	4.67	4.67	4.67	4.67	4.67	4.67	4.67	3.67	4.33	4.00	3.67	3.67	3.67	3.33
	night						morning						afternoon						evening					

(**c**)

Figure 7. RMA-based risk profiles for: (**a**) increasing temperature risk; (**b**) air pollution risk; (**c**) combination of increasing temperature and air pollution (multi-risk).

Finally, Figure 8 resumes the daily evolution of the multi-risk scenarios for morning, afternoon, evening, and night scenarios, overlapping the cadastral maps of the selected case studies and the risk levels obtained through the matrix. Supplementary Material Video S1 resumes a time-dependent visualization of daily variation of the risk for the multi-hazard combinations according to the same meso-scale maps approach.

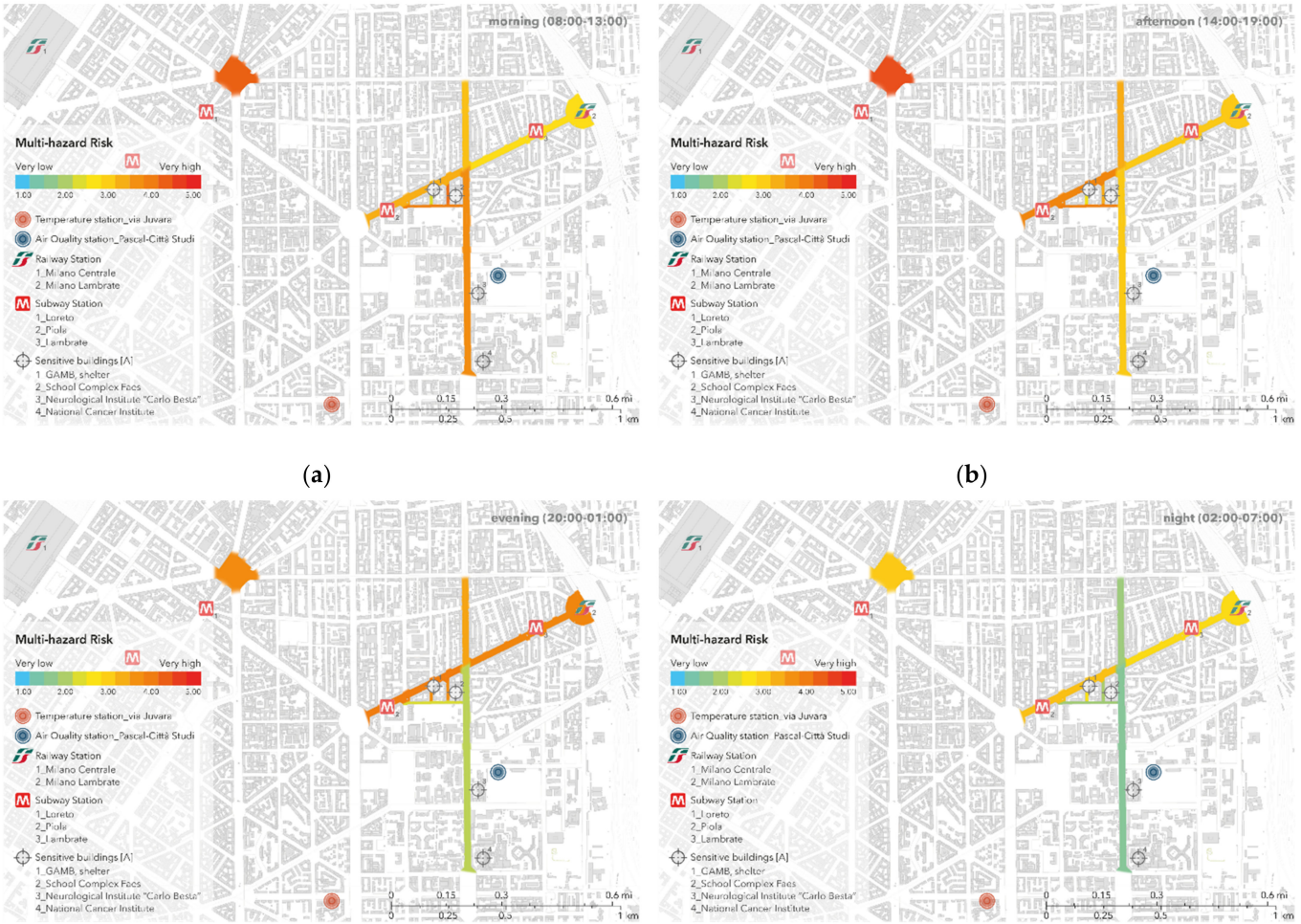

(**a**) (**b**)

(**c**) (**d**)

Figure 8. Meso-scale maps of multi-risk for: (**a**) morning scenario; (**b**) afternoon scenario; (**c**) evening scenario; (**d**) night scenario.

4. Discussion

This work provides an innovative and quick-to-apply method for defining a BE-oriented pedestrian risk index in the context of heat waves and air pollution in urban BEs. Its applicability has been tested thanks to some relevant BEs in the city of Milan, Italy. The results identify main key findings about (1) the case studies application, (2) the capability demonstration in view of risk assessment tasks for stakeholders and (3) the support of risk mitigation strategies proposal.

Considering the case study application, the procedure identifies the risk from single-risk and a multi-risk perspectives, demonstrating that the considered risk factors imply a variety of risk conditions over time and meso-scale spaces. The results show that the core hours of the day are the most at risk. In such a scenario, considering the residents' habits assumed in this work, pedestrians can be mainly represented by the elderly, babies and young people, thus increasing the multi-risk level since they are the most prone users' typologies to suffer the effects of both increasing temperature and air pollution.

The morphology of the BE influences the relative effects of SLODs on the microclimate and pedestrians. More specifically, the spatial distribution of buildings, the presence of commercial activities and public services, the presence of green infrastructure, and the layout and morphology of roads have a strong influence on the chosen means of transport and the intensity of human activities, social interactions, and pedestrian behaviour. In this sense, the results (i.e., see Section 3.3) show that Piazzale Loreto is the riskiest BE from single- and multi-risk perspectives, and considering all the daytime, essentially because of the total absence of shady areas and green infrastructure together with heavy traffic levels. Via Pacini or Via Ponzio have similar traffic conditions to those in Piazzale Loreto, and they are also affected by the presence of sensitive buildings, but the risk is lower because of the morphological characteristics of the BE and the presence of green infrastructure.

Considering impacts on risk assessment tasks for stakeholders, the proposed methodology has been defined to allow risk analysis quickly also by non-expert or low-trained technicians (including those of local authorities such as municipalities). Stakeholders and decision makers can follow the overall framework of Figure 1 to evaluate the current scenario and its "hot-spots". Although the case study of Milan has been supported by organized databases, the method takes advantage of easy-to-collect variables using open-data and freely accessible databases (online), thus also improving existing approaches [2,11,25,26,37]. In this sense, the results seem to succeed in developing the following issues:

1. The data collected have been processed to obtain a series of synthetic criteria, easily interpretable and adaptable to any type of urban BE, as they can be derived using commonly used tools such as Google Maps. For example, green infrastructure can be assessed by observing the BE using Google Street View and noting the criteria outlined in Table 2.
2. Matrix scale assessments (RMA) enable comparing the same AS/LS or several ASs/LSs in terms of specific features (i.e., each risk factor, and each parameter concerning vulnerability and exposure) and their response to SLODs (in a single and multi-risk perspective). In this sense, the method focuses on the aspects characterizing pedestrian risk, as it relies on the characterization of the space where pedestrians move and on the possible quantity of pedestrians using the BE.
3. The parameters of the method can be further explored to create scenarios that can be analysed in more detail with simulation tools, both oriented towards pedestrian dynamics and SLODs modelling.
4. In view of point 3, the single-risk-oriented assessment can allow decision makers (i.e., local authorities) to understand which of the two SLODs is more impactful in the analysed context, thus being able to address future risk-mitigation strategies. Similarly, the multi-hazard assessment can help them to recognize which of the ASs or LSs being analysed is the most risky and to identify the most appropriate response for each case. Nevertheless, a full comparison of the different ASs/LSs should shift from normalizing the exposure for each BE to normalizing the exposure for the maximum

exposure in the BEs to be compared. In this case, the normalization of the exposure could take advantage of the pedestrian density in the outer areas, thereby having a single reference value for all the BE.

As noted in point 4, this work has significant implications, while considering the support of the proposed risk mitigation strategy. In fact, the implementation of risk-reduction strategies in the BEs can be mainly associated with a variation in the related physical vulnerability classes (e.g., intervention on green infrastructure by introducing green walls and/or green roofs; interventions regulating traffic levels or boosting urban public transport) [8]. Similarly, exposure- and social-vulnerability-related interventions could limit the critical interaction between pedestrians and risky BEs, such as rethinking the use of sensitive buildings (e.g., such as hospitals or clinics) by also relocating them to other BEs if possible, or regulating other attractive urban spaces (e.g., shopping centres, shops, railway stations, etc.) to control the exposure of pedestrians. In this sense, the proposed risk assessment method (and of the related risk indexes) can be used to simulate future risk scenarios characterized by new specific conditions of the considered parameters. The variation in parameters will depend on specific urban regeneration and renewal interventions, in order to improve meso-scale risk in a long-term planning perspective. Such analysis could also take advantage of predictive models for future trends in the assessed SLODs in urban BEs, such as those relating to pollution and UTCI simulation in the urban fabric. Considering all these cases, the proposed method can then be used to assess the impact of these strategies on single and multi-risk of the BEs. To this end, other activities could correlate single and multi-risk indexes of specific health problems for pedestrians, in order to better transition from general tasks to specific risk assessment. In this case, the decision makers' support will also imply the analysis of health outcomes on the population, thus linking a BE-oriented perspective to management and clinical analysis that can be useful at a whole urban or regional level.

The authors are aware of limitations to the work that could be solved by future research steps. Although the data collected for the city of Milan allowed a mesoscopic analysis of risk conditions, future research should evaluate the main following issues to improve the reliability of the performed analysis:

- The possibility of updating pollutant concentration and weather data through direct detection campaigns for each case study, including microscopic hazard assessment. In this sense, the approach proposed by this work can be also used by adopting a grid for the urban BE representation (e.g., 5 m $\times$ 5 m; 10 m $\times$ 10 m). This means that all the risk factors and parameters must be micro-scaled to note differences in the same AS/LS without changing the overall methodological approach.
- The integration of in situ analysis and measurements to improve the reliability of data on the specific scenario, or even their substitution with data collection from exclusively open source materials (i.e., Google Maps and Streetview), which are likely available in much of the industrialized world but that may not be so readily available in other countries. In particular:
    a. Introduce more information than the typical traffic fleet of the area analysed (vehicle type, power type, etc.).
    b. Use in situ analysis for pedestrian traffic level to improve the quantification of possible flows over the daytime, rather than using conservative but simplified assessment assumptions (i.e., "all the building occupants can be potential pedestrians at each time of the day").
    c. In situ measurements to estimate actual albedo values, to consider separately the materiality and climatic characteristics of the analysed area. The use of the UTCI can be similar for different areas with diverse materiality and weather conditions, but not analysing them separately hinders planning and selecting mitigation strategies.

- Define different priorities in the risk-assessment tasks and goals by the decay managers who conduct different scenarios analyses using the AHP methodology. In fact, the AHP integration in the whole framework allows one to quantitatively assess the consistency of weights of the factors depending on the initial (e.g., literature-based) assumptions. For instance, the multi-risk index weights can be varied depending on the priority goals to be faced in the urban BE.
- Introduce additional social vulnerability factors rather than the sensitivity towards the SLOD effects, to include social, economic and cultural issues affecting the individual available resources to face ill effects of the environment.
- Introduce different exposure and social vulnerability scenarios, rather than using peak exposure and statistics on age at the whole district level. In this sense, probabilistic approaches could also be used to evaluate variations in the number of people in the BEs. Since this work relies on the assessment of typical working days, future works could apply the method to other typical scenarios to consider such as the weekend or holiday periods, during which user habits can be very different from the working days and business activities have different opening hours. Furthermore, these study conditions could be influenced by the contextual conditions in which the analysis was performed, i.e., restrictions to contain the COVID-19 pandemic that severely impacted pedestrians' freedom of movement.

5. Conclusions

Pedestrians in urban built environments (BEs) are increasingly at risk from SLODs, such as air pollution and increasing temperature, also given the increasing importance that the open spaces of the BE have acquired in the last period for social relationships. In recent years, the exposure of pedestrians to increasing temperature and air pollution has resulted in a general worsening of individual health conditions, especially for people of frail health. The effectiveness of risk mitigation solutions should be defined and verified in relation to specific scenarios in terms of morphology, environment and user-related problems. Thus, quick but reliable methods of risk assessment methods for such scenarios from single- and multi-risk perspectives are urgently required.

This study proposes a methodology to evaluate single- and multi-risk areal spaces (ASs) and linear spaces (LSs) in the urban fabric due to such SLODs, using an expeditious approach, easily available data and recognised demographic groups. The applicability and robustness of the whole methodological framework have been demonstrated through a case study application, highlighting its flexibility and ease of data collection and management of exposure, vulnerability and, then, risk, through the use of a risk matrix that combines quantitative and qualitative data. In particular, physical vulnerability was introduced taking into account the differentiated BE response to SLODs. The exposure was calculated according to the functional occupying density of the space of the buildings and the open spaces present. The social vulnerability was introduced using weights based on the fragility of certain demographic groups, and the risk was calculated using a risk matrix, combining the results obtained previously.

Being able to define critical hazard-exposure scenarios from input data, the proposed methodology can also be used as a support tool to define risk mitigation strategies, giving priority interventions relating to urban BE design and regeneration (e.g., using the implementation of risk-reducing components in buildings and outdoor surfaces; using pedestrian and traffic management strategies). Thus, this work contributes to a move towards a more resilient, sustainable, and safe city, capable of facing future social and environmental challenges, including the reconversion of the post-pandemic BEs to the challenges due to climate change and air pollution.

Supplementary Materials: The following supporting information can be downloaded at: https://www.mdpi.com/article/10.3390/su141811233/s1; Video S1: Meso-scale maps of daily variation of the risk (multi-hazard combination).

Author Contributions: Conceptualization, E.Q., G.B., G.S. (Graziano Salvalai) and J.D.B.C.; methodology, E.Q., G.B., G.S. (Graziano Salvalai), G.S. (Gessica Sparvoli) and J.D.B.C.; data curation, G.S. (Gessica Sparvoli) and J.D.B.C.; validation, G.B., G.S. (Gessica Sparvoli) and J.D.B.C.; formal analysis, G.B., G.S. (Gessica Sparvoli) and J.D.B.C.; investigation, G.B., G.S. (Gessica Sparvoli) and J.D.B.C.; resources, G.S. (Graziano Salvalai) and J.D.B.C.; writing—original draft preparation, E.Q., G.B., G.S. (Graziano Salvalai), G.S. (Gessica Sparvoli) and J.D.B.C.; writing—review and editing, E.Q., G.B., G.S. (Graziano Salvalai), G.S. (Gessica Sparvoli) and J.D.B.C.; visualization, G.S. (Gessica Sparvoli); supervision, E.Q. and G.S. (Graziano Salvalai); project administration, E.Q. and G.S. (Graziano Salvalai); funding acquisition, E.Q. and G.S. (Graziano Salvalai). All authors have read and agreed to the published version of the manuscript.

Funding: This research was funded by the MIUR (the Italian Ministry of Education, University, and Research) Project BE S2ECURe—(make) Built Environment Safer in Slow and Emergency Conditions through behavioural assessed/designed Resilient solutions (Grant number: 2017LR75XK).

Institutional Review Board Statement: Not applicable.

Informed Consent Statement: Not applicable.

Data Availability Statement: Original repositories on the original (raw) data are included in the text in relation to each of the assessed aspects. Elaborated data that support the findings of this study are available from the corresponding author upon reasonable request.

Conflicts of Interest: The authors declare no conflict of interest.

References

1. Siegele, L. *Loss and Damage: The Theme of Slow Onset Impact, Loss & Damage in Vulnerable Countries Initiative, Climate Development Knowledge Network*; Germanwatch: Berlin, Germany, 2012; Volume 1.
2. Lee, J.; Kim, D.; Park, J. A Machine Learning and Computer Vision Study of the Environmental Characteristics of Streetscapes That Affect Pedestrian Satisfaction. *Sustainability* **2022**, *14*, 5730. [CrossRef]
3. Jabbari, M.; Fonseca, F.; Ramos, R. Accessibility and Connectivity Criteria for Assessing Walkability: An Application in Qazvin, Iran. *Sustainability* **2021**, *13*, 3648. [CrossRef]
4. Yang, J.; Shi, B.; Zheng, Y.; Shi, Y.; Xia, G. Urban Form and Air Pollution Disperse: Key Indexes and Mitigation Strategies. *Sustain. Cities Soc.* **2020**, *57*, 101955. [CrossRef]
5. Pigliautile, I.; Marseglia, G.; Pisello, A.L. Investigation of CO_2 Variation and Mapping Through Wearable Sensing Techniques for Measuring Pedestrians' Exposure in Urban Areas. *Sustainability* **2020**, *12*, 3936. [CrossRef]
6. Abigail, W.; Jonathan, G.; Herriet, E. The Toxic School Run. Report written by Harriet Edwards, Unicef UK, and Dr. Abigail Whitehouse, QMUL. 2018. Available online: https://www.unicef.org.uk/publications/the-toxic-school-run/ (accessed on 6 September 2022).
7. Miao, C.; Yu, S.; Hu, Y.; Bu, R.; Qi, L.; He, X.; Chen, W. How the Morphology of Urban Street Canyons Affects Suspended Particulate Matter Concentration at the Pedestrian Level: An in-Situ Investigation. *Sustain. Cities Soc.* **2020**, *55*, 102042. [CrossRef]
8. Tomson, M.; Kumar, P.; Barwise, Y.; Perez, P.; Forehead, H.; French, K.; Morawska, L.; Watts, J.F. Green Infrastructure for Air Quality Improvement in Street Canyons. *Environ. Int.* **2021**, *146*, 106288. [CrossRef]
9. Oke, T.R. The Urban Energy Balance. *Prog. Phys. Geogr. Earth Environ.* **1988**, *12*, 471–508. [CrossRef]
10. Arnfield, A.J. Two Decades of Urban Climate Research: A Review of Turbulence, Exchanges of Energy and Water, and the Urban Heat Island. *Int. J. Climatol.* **2003**, *23*, 1–26. [CrossRef]
11. Blanco Cadena, J.D.; Salvalai, G.; Lucesoli, M.; Quagliarini, E.; D'Orazio, M. Flexible Workflow for Determining Critical Hazard and Exposure Scenarios for Assessing SLODs Risk in Urban Built Environments. *Sustainability* **2021**, *13*, 4538. [CrossRef]
12. Salvalai, G.; Grecchi, M.; Poli, T.; Cecconi, F.R.; Malighetti, L.; Diego, J.; Cadena, B.; Moretti, N.; Beatrice, O. WP 2-BE and SLOD: SoA, Risks and Human Behavior T.2.1-SoA-Based Definition and Characterization of BE as Network of Buildings, Infrastructures, Connecting Space in Reference to SLOD Occurrence and Users' Typologies DELIVERABLE ID D.2.1.1-Built Environment Prone to SLOD Definition. 2019. Available online: https://www.bes2ecure.net/_files/ugd/ac84c9_87d628ee84384438b1685a712cb1ddad.pdf (accessed on 6 September 2022).
13. De Nazelle, A.; Rodríguez, D.A.; Crawford-Brown, D. The Built Environment and Health: Impacts of Pedestrian-Friendly Designs on Air Pollution Exposure. *Sci. Total Environ.* **2009**, *407*, 2525–2535. [CrossRef] [PubMed]
14. Sharifi, A. Urban Form Resilience: A Meso-Scale Analysis. *Cities* **2019**, *93*, 238–252. [CrossRef]
15. Amirzadeh, M.; Sobhaninia, S.; Sharifi, A. Urban Resilience: A Vague or an Evolutionary Concept? *Sustain. Cities Soc.* **2022**, *81*, 103853. [CrossRef]
16. Ghobadi, P.; Nasrollahi, N. Assessment of Pollutant Dispersion in Deep Street Canyons under Different Source Positions: Numerical Simulation. *Urban Clim.* **2021**, *40*, 101027. [CrossRef]

17. De Jesus, M.C.R.; Rodrigues da Silva, A.N. Barrier Effect in a Medium-Sized Brazilian City: An Exploratory Analysis Using Decision Trees and Random Forests. *Sustainability* **2022**, *14*, 6309. [CrossRef]
18. Fonseca, F.; Conticelli, E.; Papageorgiou, G.; Ribeiro, P.; Jabbari, M.; Tondelli, S.; Ramos, R. Levels and Characteristics of Utilitarian Walking in the Central Areas of the Cities of Bologna and Porto. *Sustainability* **2021**, *13*, 3064. [CrossRef]
19. Sharifi, A. Resilient Urban Forms: A Review of Literature on Streets and Street Networks. *Build. Environ.* **2019**, *147*, 171–187. [CrossRef]
20. Koren, D.; Rus, K. The Potential of Open Space for Enhancing Urban Seismic Resilience: A Literature Review. *Sustainability* **2019**, *11*, 5942. [CrossRef]
21. La Rosa, D.; Pappalardo, V. Planning for Spatial Equity—A Performance Based Approach for Sustainable Urban Drainage Systems. *Sustain. Cities Soc.* **2020**, *53*, 101885. [CrossRef]
22. Bernardini, G.; Ferreira, T.M. Emergency and Evacuation Management Strategies in Earthquakes: Towards Holistic and User-Centered Methodologies for Their Design and Evaluation. In *Seismic Vulnerability Assessment of Civil Engineering Structures at Multiple Scales*; Elsevier: Amsterdam, The Netherlands, 2022; pp. 275–321.
23. BE S2ECURE Project D 2.2.5 | Matrix of SLOD Risk Condition; 2020; Working Report (draft) from BE S2ECURe "(Make) Built Environment Safer in Slow and Emergency Conditions through Behavioural Assessed/Designed Resilient Solutions" Research Project. Available online: https://bit.ly/3yyVdfj (accessed on 31 May 2022).
24. Polednik, B.; Piotrowicz, A. Pedestrian Exposure to Traffic-Related Particles along a City Road in Lublin, Poland. *Atmos. Pollut. Res.* **2020**, *11*, 686–692. [CrossRef]
25. Abrar, R.; Sarkar, S.K.; Nishtha, K.T.; Talukdar, S.; Shahfahad; Rahman, A.; Islam, A.R.M.T.; Mosavi, A. Assessing the Spatial Mapping of Heat Vulnerability under Urban Heat Island (UHI) Effect in the Dhaka Metropolitan Area. *Sustainability* **2022**, *14*, 4945. [CrossRef]
26. Steeneveld, G.-J.; Klompmaker, J.O.; Groen, R.J.A.; Holtslag, A.A.M. An Urban Climate Assessment and Management Tool for Combined Heat and Air Quality Judgements at Neighbourhood Scales. *Resour. Conserv. Recycl.* **2018**, *132*, 204–217. [CrossRef]
27. Available online: http://www.utci.org/ (accessed on 14 June 2022).
28. Available online: https://www.airnow.gov/aqi/aqi-basics/#:~{}:text=think%20of%20the%20aqi%20as,300%20represents%20hazardous%20air%20quality (accessed on 14 June 2022).
29. Villagran De Leon, J. *Vulnerability: A Conceptual and Methodological Review*; UNU-EHS: Bonn, Germany, 2006; Volume 4.
30. Choi, Y.; Yoon, H.; Kim, D. Where Do People Spend Their Leisure Time on Dusty Days? Application of Spatiotemporal Behavioral Responses to Particulate Matter Pollution. *Ann. Reg. Sci.* **2019**, *63*, 317–339. [CrossRef]
31. D'Amato, G.; Holgate, S.T.; Pawankar, R.; Ledford, D.K.; Cecchi, L.; Al-Ahmad, M.; Al-Enezi, F.; Al-Muhsen, S.; Ansotegui, I.; Baena-Cagnani, C.E.; et al. Meteorological Conditions, Climate Change, New Emerging Factors, and Asthma and Related Allergic Disorders. A Statement of the World Allergy Organization. *World Allergy Organ. J.* **2015**, *8*, 1–52. [CrossRef]
32. Morais, L.; Lopes, A.; Nogueira, P. Human Health Outcomes at the Neighbourhood Scale Implications: Elderly's Heat-Related Cardiorespiratory Mortality and Its Influencing Factors. *Sci. Total Environ.* **2021**, *760*, 144036. [CrossRef]
33. Vanos, J.K. Children's Health and Vulnerability in Outdoor Microclimates: A Comprehensive Review. *Environ. Int.* **2015**, *76*, 1–15. [CrossRef]
34. Devlin, R.B.; Ghio, A.J.; Kehrl, H.; Sanders, G.; Cascio, W. Elderly Humans Exposed to Concentrated Air Pollution Particles Have Decreased Heart Rate Variability. *Eur. Respir. J.* **2003**, *21*, 76S–80S. [CrossRef]
35. Cakmak, S.; Dales, R.E.; Vidal, C.B. Air Pollution and Mortality in Chile: Susceptibility among the Elderly. *Environ. Health Perspect.* **2007**, *115*, 524–527. [CrossRef]
36. Delfino, R.J.; Tjoa, T.; Gillen, D.L.; Staimer, N.; Polidori, A.; Arhami, M.; Jamner, L.; Sioutas, C.; Longhurst, J. Traffic-Related Air Pollution and Blood Pressure in Elderly Subjects with Coronary Artery Disease. *Epidemiology* **2010**, *21*, 396–404. [CrossRef]
37. Blanco Cadena, J.D.; Moretti, N.; Salvalai, G.; Quagliarini, E.; Re Cecconi, F.; Poli, T. A New Approach to Assess the Built Environment Risk under the Conjunct Effect of Critical Slow Onset Disasters: A Case Study in Milan, Italy. *Appl. Sci.* **2021**, *11*, 1186. [CrossRef]
38. Jia, Y.-P.; Lu, K.-F.; Zheng, T.; Li, X.-B.; Liu, X.; Peng, Z.-R.; He, H.-D. Effects of Roadside Green Infrastructure on Particle Exposure: A Focus on Cyclists and Pedestrians on Pathways between Urban Roads and Vegetative Barriers. *Atmos. Pollut. Res.* **2021**, *12*, 1–12. [CrossRef]
39. Zhu, Q.; Kuang, X.; Shen, Y. Risk Matrix Method and Its Application in the Field of Technical Project Risk Management. *Eng. Sci.* **2003**, *5*, 89–94.
40. Ni, H.; Chen, A.; Chen, N. Some Extensions on Risk Matrix Approach. *Saf. Sci.* **2010**, *48*, 1269–1278. [CrossRef]
41. Kortetmäki, T.; Järvelä, M. Social Vulnerability to Climate Policies: Building a Matrix to Assess Policy Impacts on Well-Being. *Environ. Sci. Policy* **2021**, *123*, 220–228. [CrossRef]
42. Leal Filho, W.; Echevarria Icaza, L.; Neht, A.; Klavins, M.; Morgan, E.A. Coping with the Impacts of Urban Heat Islands. A Literature Based Study on Understanding Urban Heat Vulnerability and the Need for Resilience in Cities in a Global Climate Change Context. *J. Clean. Prod.* **2018**, *171*, 1140–1149. [CrossRef]
43. Linch, K. *The Image of the City*; MIT Press: Cambridge, MA, USA, 1960; ISBN 978-0262120043.
44. Vardoulakis, S.; Fisher, B.E.A.; Pericleous, K.; Gonzalez-Flesca, N. Modelling Air Quality in Street Canyons: A Review. *Atmos. Environ.* **2003**, *37*, 155–182. [CrossRef]

45. Zheng, T.; Jia, Y.-P.; Zhang, S.; Li, X.-B.; Wu, Y.; Wu, C.-L.; He, H.-D.; Peng, Z.-R. Impacts of Vegetation on Particle Concentrations in Roadside Environments. *Environ. Pollut.* **2021**, *282*, 117067. [CrossRef]
46. Martins, T.A.L.; Adolphe, L.; Bonhomme, M.; Bonneaud, F.; Faraut, S.; Ginestet, S.; Michel, C.; Guyard, W. Impact of Urban Cool Island Measures on Outdoor Climate and Pedestrian Comfort: Simulations for a New District of Toulouse, France. *Sustain. Cities Soc.* **2016**, *26*, 9–26. [CrossRef]
47. Guo, Z.; Li, B.; Hovestadt, L. Urban Traffic Modeling and Pattern Detection Using Online Map Vendors and Self-Organizing Maps. *Front. Archit. Res.* **2021**, *10*, 715–728. [CrossRef]
48. De Lotto, R.; Pietra, C.; Venco, E.M. Risk Analysis: A Focus on Urban Exposure Estimation. In *Computational Science and Its Applications*; Lecture Notes in Computer Science; Springer: Cham, Switzerland, 2019; Volume 11620. [CrossRef]
49. Available online: https://www.emdat.be/ (accessed on 28 June 2022).
50. European Court of Auditors. Air Pollution: Our Health Still Insufficiently Protected. 2018. Available online: https://op.europa.eu/webpub/eca/special-reports/air-quality-23-2018/en/#chapter8 (accessed on 6 September 2022).
51. Available online: https://Ipccitalia.Cmcc.It/ (accessed on 21 June 2022).
52. Available online: https://www.comune.milano.it/ (accessed on 17 June 2022).
53. Available online: https://www.google.it/maps/place/milano+mi/@45.4627124,9.1076923,12z/data=!3m1!4b1!4m5!3m4!1s0x4786c1493f1275e7:0x3cffcd13c6740e8d!8m2!3d45.4642242!4d9.1900635 (accessed on 17 June 2022).
54. Available online: https://www.openstreetmap.org/#map=17/45.48061/9.22722 (accessed on 17 June 2022).
55. D.m. n.6792 Del 05/11/2001. Available online: https://www.mit.gov.it/normativa/decreto-ministeriale-protocollo-6792-del-05112001 (accessed on 17 June 2022).
56. National Academies of Sciences, Engineering, and Medicine. *Highway Capacity Manual (HCM) 7th Edition: A Guide for Multimodal Mobility Analysis*; The National Academies Press: Washington, DC, USA, 2022. [CrossRef]
57. Available online: https://www.acgih.org/ (accessed on 17 June 2022).
58. Available online: https://www.epa.gov/ (accessed on 17 June 2022).
59. Abdulateef, M.F.; Al-Alwan, A.S.H. The Effectiveness of Urban Green Infrastructure in Reducing Surface Urban Heat Island. *Ain Shams Eng. J.* **2021**, *13*, 101526. [CrossRef]
60. Li, P.; Wang, Z.-H. Environmental Co-Benefits of Urban Greening for Mitigating Heat and Carbon Emissions. *J. Environ. Manag.* **2021**, *293*, 112963. [CrossRef]
61. Pioppi, B.; Pigliautile, I.; Pisello, A.L. Human-Centric Microclimate Analysis of Urban Heat Island: Wearable Sensing and Data-Driven Techniques for Identifying Mitigation Strategies in New York City. *Urban Clim.* **2020**, *34*, 100716. [CrossRef]
62. Karimimoshaver, M.; Khalvandi, R.; Khalvandi, M. The Effect of Urban Morphology on Heat Accumulation in Urban Street Canyons and Mitigation Approach. *Sustain. Cities Soc.* **2021**, *73*, 103127. [CrossRef]
63. Yang, H.; Chen, G.; Wang, D.; Hang, J.; Li, Q.; Wang, Q. Influences of Street Aspect Ratios and Realistic Solar Heating on Convective Heat Transfer and Ventilation in Full-Scale 2D Street Canyons. *Build. Environ.* **2021**, *204*, 108125. [CrossRef]
64. Sun, J.; Liu, H.; Ma, Z. Modelling and Simulation of Highly Mixed Traffic Flow on Two-Lane Two-Way Urban Streets. *Simul. Model. Pract. Theory* **2019**, *95*, 16–35. [CrossRef]
65. Zhu, L.; Ranasinghe, D.; Chamecki, M.; Brown, M.J.; Paulson, S.E. Clean Air in Cities: Impact of the Layout of Buildings in Urban Areas on Pedestrian Exposure to Ultrafine Particles from Traffic. *Atmos. Environ.* **2021**, *252*, 118267. [CrossRef]
66. Abhijith, K.V.; Kumar, P.; Gallagher, J.; McNabola, A.; Baldauf, R.; Pilla, F.; Broderick, B.; di Sabatino, S.; Pulvirenti, B. Air Pollution Abatement Performances of Green Infrastructure in Open Road and Built-up Street Canyon Environments—A Review. *Atmos. Environ.* **2017**, *162*, 71–86. [CrossRef]
67. Macintyre, H.L.; Heaviside, C.; Taylor, J.; Picetti, R.; Symonds, P.; Cai, X.-M.; Vardoulakis, S. Assessing Urban Population Vulnerability and Environmental Risks across an Urban Area during Heatwaves—Implications for Health Protection. *Sci. Total Environ.* **2018**, *610–611*, 678–690. [CrossRef]
68. Ellena, M.; Breil, M.; Soriani, S. The Heat-Health Nexus in the Urban Context: A Systematic Literature Review Exploring the Socio-Economic Vulnerabilities and Built Environment Characteristics. *Urban Clim.* **2020**, *34*, 100676. [CrossRef]
69. Mao, H.; Fan, X.; Guan, J.; Chen, Y.-C.; Su, H.; Shi, W.; Zhao, Y.; Wang, Y.; Xu, C. Customer Attractiveness Evaluation and Classification of Urban Commercial Centers by Crowd Intelligence. *Comput. Hum. Behav.* **2019**, *100*, 218–230. [CrossRef]
70. Fraser, A.M.; Chester, M.V.; Eisenman, D. Strategic Locating of Refuges for Extreme Heat Events (or Heat Waves). *Urban Clim.* **2018**, *25*, 109–119. [CrossRef]
71. Liang, S.; Leng, H.; Yuan, Q.; Wang, B.; Yuan, C. How Does Weather and Climate Affect Pedestrian Walking Speed during Cool and Cold Seasons in Severely Cold Areas? *Build. Environ.* **2020**, *175*, 106811. [CrossRef]
72. Piano Nazionale Di Prevenzione Degli Effetti Del Caldo Sulla Salute—Linee Di Indirizzo per La Prevenzione. Report 2019. Available online: https://www.salute.gov.it/imgs/C_17_pubblicazioni_2867_allegato.pdf (accessed on 6 September 2022).
73. D.Lgs. n.114 Del 98—Riforma Della Disciplina Relativa al Settore Del Commercio. Available online: https://www.bosettiegatti.eu/info/norme/statali/1998_0114.htm (accessed on 6 September 2022).
74. Bloomberg, B. New York City Pedestrian Level of Service Study Phase I; New York. 2006. Available online: https://www1.nyc.gov/assets/planning/download/pdf/plans/transportation/td_fullpedlosb.pdf (accessed on 6 September 2022).
75. Available online: https://planningtank.com/transportation/level-of-service (accessed on 17 June 2022).
76. Available online: https://bpmsg.com/ahp/ahp-calc.php (accessed on 17 June 2022).

77. Available online: https://www.dati.lombardia.it/ambiente/mappa-stazioni-meteorologiche/8ux9-ue3c (accessed on 21 June 2022).
78. Available online: https://www.arpalombardia.it/pages/aria/qualita-aria.aspx (accessed on 21 June 2022).
79. Available online: https://geoportale.comune.milano.it/portal/apps/webappviewer/index.html?id=3fbcdc3d3e6449918f73a3840d519798 (accessed on 17 June 2022).
80. Available online: https://geoportale.comune.milano.it/mapviewerapplication/map/app?config=%2fmapviewerapplication%2fmap%2fconfig4app%2f477&id=ags (accessed on 17 June 2022).
81. Jasiński, A. COVID-19 Pandemic Is Challenging Some Dogmas of Modern Urbanism. *Cities* **2021**, *121*, 103498. [CrossRef]
82. Corazza, M.V.; Moretti, L.; Forestieri, G.; Galiano, G. Chronicles from the New Normal: Urban Planning, Mobility and Land-Use Management in the Face of the COVID-19 Crisis. *Transp. Res. Interdiscip. Perspect.* **2021**, *12*, 100503. [CrossRef]
83. Available online: http://sisi.comune.milano.it/ (accessed on 5 July 2022).